The Differences Between *Cis*- and *Trans*-Gene Inactivation Caused by Heterochromatin in *Drosophila*

Yuriy A. Abramov,*,[1] Aleksei S. Shatskikh,*,[1] Oksana G. Maksimenko,† Silvia Bonaccorsi,‡ Vladimir A. Gvozdev,*,[2] and Sergey A. Lavrov*,[2]

*Department of Molecular Genetics of the Cell, Institute of Molecular Genetics, Russian Academy of Science, Moscow 123182, Russia, and †Institute of Gene Biology, Russian Academy of Sciences, 119334 Moscow, Russia, and ‡Department of Biology and Biotechnology "Charles Darwin," Sapienza University of Rome, 00185, Italy

ABSTRACT Position-effect variegation (PEV) is the epigenetic disruption of gene expression near the *de novo*–formed euchromatin-heterochromatin border. Heterochromatic *cis*-inactivation may be accompanied by the *trans*-inactivation of genes on a normal homologous chromosome in *trans*-heterozygous combination with a PEV-inducing rearrangement. We characterize a new genetic system, inversion *In(2)A4*, demonstrating *cis*-acting PEV as well as *trans*-inactivation of the reporter transgenes on the homologous nonrearranged chromosome. The *cis*-effect of heterochromatin in the inversion results not only in repression but also in activation of genes, and it varies at different developmental stages. While *cis*-actions affect only a few juxtaposed genes, *trans*-inactivation is observed in a 500-kb region and demonstrates a nonuniform pattern of repression with intermingled regions where no transgene repression occurs. There is no repression around the histone gene cluster and in some other euchromatic sites. *trans*-Inactivation is accompanied by dragging of euchromatic regions into the heterochromatic compartment, but the histone gene cluster, located in the middle of the *trans*-inactivated region, was shown to be evicted from the heterochromatin. We demonstrate that *trans*-inactivation is followed by *de novo* HP1a accumulation in the affected transgene; *trans*-inactivation is specifically favored by the chromatin remodeler SAYP and prevented by Argonaute AGO2.

KEYWORDS heterochromatin; *Drosophila*; PEV; *trans*-inactivation; nuclear compartmentalization

Position-effect variegation (PEV) is an epigenetic phenomenon of inactivation of a gene in a portion of cells caused by relocation of a gene into or very close to the heterochromatin. Heterochromatin has a distinct chromatin structure that includes specific histone modifications, associated proteins, and a condensed nucleosome package. This structure can spread from the euchromatin-heterochromatic border into the euchromatin by self-assembly and propagation of a complex containing SU(VAR)3-9 histone methyltransferase, HP1a, and SU(VAR)3-7 proteins, thus affecting the expression of euchromatic genes near the border (Grewal and Elgin 2002; Schotta *et al.* 2003; Hines *et al.* 2009; Elgin and Reuter 2013). Analysis of the spreading of heterochromatin using high-throughput approaches has been performed in a single paper aimed at the analysis of *white-mottled X*-chromosomal inversions, demonstrating PEV of the *white* gene (Vogel *et al.* 2009). It was found that HP1a propagates up to 175 kb into euchromatin from the heterochromatin border and demonstrates uneven distribution over the spreading area. Only the *white* gene among 20 measured genes in this region demonstrates decreased expression as a result of PEV.

Here we present a detailed study of the genetic system (inversion *In(2)A4*) demonstrating *cis*-effects of heterochromatin on gene expression as well as inversion-induced *trans*-inactivation of the transgenes located on the homologous nonrearranged chromosome. RNA-Seq analysis shows that only a few euchromatin genes near the breakpoint of *In(2)A4*

doi: 10.1534/genetics.115.181693
Manuscript received August 28, 2015; accepted for publication October 13, 2015; published Early Online October 22, 2015.
Supporting information is available online at www.genetics.org/lookup/suppl/doi:10.1534/genetics.115.181693/-/DC1
NGS data have been submitted to the GEO database at NCBI under accession number GSE71842.
[1]These authors contributed equally to this work.
[2]Corresponding authors: Department of Molecular Genetics of the Cell, Institute of Molecular Genetics, Russian Academy of Sciences, Moscow 123182, Russia. E-mails: gvozdev@img.ras.ru and slavrov@img.ras.ru

significantly change their expression levels, similar to *white-mottled* rearrangements (Vogel *et al.* 2009). We detected not only the repression but also the activation of euchromatic genes as the *cis*-effect of inversion. We also found that *cis*-effects of heterochromatin on a given gene depend on developmental stage. To our knowledge, these peculiar *cis*-effects of heterochromatin on the adjacent euchromatic region have not been reported previously, while the phenomenon of discontinuous heterochromatinization of euchromatic regions near the breakpoint has been discussed (Talbert and Henikoff 2006).

In contrast to relatively weak *cis*-effects, the inversion *In(2)A4* causes strong and widespread inactivation of the *mini-white* reporter in transgenes on homologous nonrearranged chromosomes [preliminary data in Abramov *et al.* (2011)]. Only a few examples of *trans*-action of heterochromatin have been reported to date, and the most extensively studied case of heterochromatin-induced *trans*-inactivation is the bw^D allele induced by insertion of a satellite DNA fragment into the coding region of the *brown* gene (Sage *et al.* 2005). Both *In(2)A4* and bw^D are able to repress the *mini-white*-containing transgenes on a homologous chromosome by dragging these region into the heterochromatic compartment. Unlike bw^D, *In(2)A4* is the inversion causing significant perturbation of chromosome organization. In combination with the wild-type chromosome, it forms a loop as a result of homolog pairing and the sticking together of the separated heterochromatin block and the main pericentromeric heterochromatin. Spatial organization of the loop in the nuclear compartment appears to be the reason for the complex pattern of *trans*-inactivation that includes the noninactivated region of the histone gene cluster.

cis-Effects of heterochromatin on neighbor genes in a rearranged chromosome and *trans*-inactivation of transgenes are considered to be independent processes because the transgene can be inactivated, while a gene at a homologous site on the rearranged *In(2)A4* chromosome may remain either unaffected or even show increased transcription. HP1a accumulation was detected at *trans*-inactivated transgenes, but not on a homologous site on the *In(2)A4* chromosome. We show the proteins specifically affecting *trans*-inactivation: chromatin remodeler SAYP enhances the repression, while the component of the small interfering RNA (siRNA) pathway and possible insulator protein AGO2 prevents it. Our data point to different molecular mechanisms of *cis*-acting PEV and *trans*-inactivation caused by *In(2)A4*.

Materials and Methods

Fly stocks

Strain *A12* was created from the $y^1\ w^{67c23}$ progenitor by introducing the *P*-element-based transgenic construction carrying the *mini-white* and *LacZ* reporter genes (Tulin *et al.* 1998). The transgene is inserted at the beginning of 5′ UTR of the *Hr39* gene (position chr2L:21237278). *A12* flies have a uniform red eye color owing to expression of the *mini-white* transgene (Figure 1C). Inversion *In(2)A4* (hereafter *A4*) was produced by X-ray irradiation of *A12* flies and screening of progeny for eye color variegation. *A4* is the inversion with the breakpoints in the left arm of chromosome *2* near the transgene position and in the pericentromeric heterochromatin. *A4/A4* flies demonstrate variegated eye color (Figure 1C), reduced viability, and female sterility. *In(2)A4(ΔP)* (hereafter *A4(ΔP)*) is the *A4* derivative with the *mini-white* transgene removed by transposase-induced precise excision. *A4(ΔP)/A4(ΔP)* flies do not contain the reporter genes *mini-white* and *LacZ* but are undistinguishable from *A4/A4* in other aspects.

Trans-Inactivation evaluation

The *trans*-inactivating ability of the *A4(ΔP)* inversion was tested over a set of *mini-white*-containing transgene insertions in the 38D–40F region of chromosome *2* (69 in total, listed in Supporting Information, Table S1). These stocks, carrying different types of transgenes, *i.e.*, *P[lacW]*, *P[EP]*, *P[EPgy2]*, *PBac[RB]*, *PBac[WH]*, *P[GT1]*, *P[wHy]*, *PBac[5HPw[+]]*, and *P[XP]*, were obtained from Bloomington and Szeged collections.

To test the susceptibility of the reporter transgene to *trans*-inactivation, crosses *w*; A4(ΔP)/CyO* females to *w*; P(w)/CyO* males were performed (here and later *P(w)* denotes a normal chromosome bearing the *mini-white* transgene in the 38D–40F region). Eye colors of the *P(w)/A4(ΔP)* and *P(w)/CyO* siblings were compared, and the degree of *trans*-inactivation for each insertion was visually estimated and ranged as no (−), weak (+), medium (++), and strong (+++) inactivation (Figure 1D).

Crosses to check the impact of position-effect modifiers

A number of mutations known to affect chromatin state were tested for their effects on *cis*- and *trans*-inactivation (listed in Table S4). *trans*-Inactivated transgenes *11127* (*P[lacW]*), *20708* (*P[EPgy2]*), and *17134* (*P[EPgy2]*) were taken for this testing and demonstrated similar responses.

To test the effect of the mutation in the gene *e(y)3* (SAYP), located on the *X* chromosome, the homozygous-viable allele $e(y)3^{u1}$ was used (Shidlovskii *et al.* 2005). The *w* e(y)3*^{u1}*/FM7; A4/CyO* females were crossed to *w*; P(w)/CyO* males. The eye phenotypes of the *w* e(y)3*^{u1}*/Y; A4/P(w)* and *e(y)3*^{u1}*/Y; P(w)/CyO* males were compared.

To test the effects of dominant *Su(var)3** mutations on chromosome *3* (in genes *Su(var)3-9*, *Su(var)3-6*, *Su(var)3-1*, and *Su(var)3-7*) (Table S4 lists the alleles), the crosses of w^{m4h}*/Y; Su(var)3*/TM3, Sb Ser* males to *yw/yw; SM1, CyRoi; TM6b, Tb* females were performed. The F_1 males *yw/Y; SM1, CyRoi; Su(var)3*/TM6b, Tb* were then crossed to females *A4/SM1, CyO; TM3, Sb Ser* to produce F_2 *yw/yw; A4/SM1, CyRoi; Su(var)3*/TM3, Sb Ser* females. These females were crossed to males *yw/Y; P(w)/SM1, CyO*. Eye colors of *yw/Y; A4/P(w); Su(var)3** and *yw/Y; P(w)/SM1, CyO; Su(var)3** males were compared.

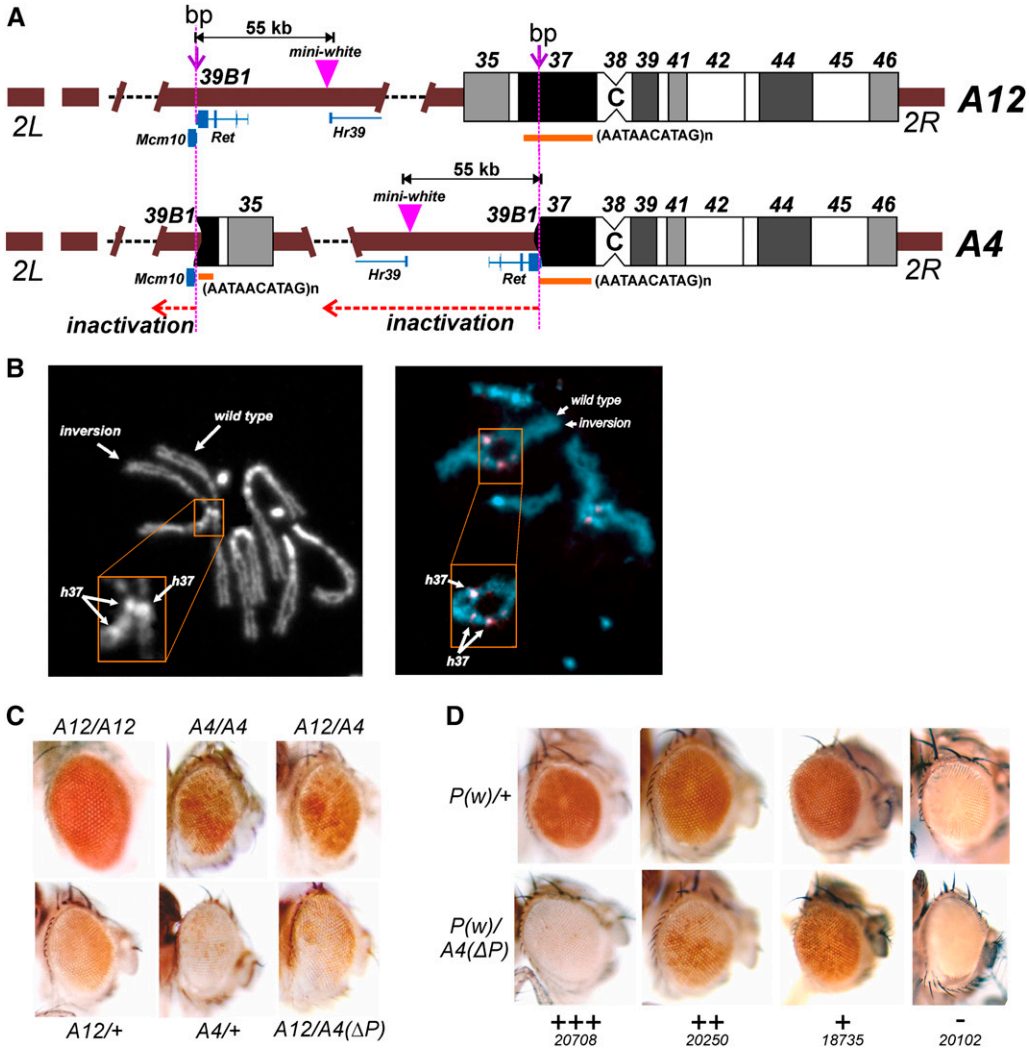

Figure 1 Structure of the *A4* rearrangement and the manifestation of *cis*- and *trans*-inactivation of *mini-white* in reporter transgenes. (A) Structure of the *A4* chromosome. Breakpoint positions (bp) in euchromatin and heterochromatin are located in the second exon of the *Mcm10* gene and in the *h37* heterochromatin block [according to Dimitri (1991)], respectively. C, centromere. The purple triangle designates the *mini-white*-containing *P*-element in the *Hr39* gene. Dashed arrows show the spreading of inactivation caused by the main heterochromatic block and the detached small block of heterochromatin. (B) Localization of the heterochromatic breakpoint in *A4*. (Left) DAPI staining of mitotic chromosomes from *A12/A4* larval brains. (Right) *In situ* hybridization using the $(AATAACATAG)_n$ probe (red). The positions of the *h37* block are marked on chromosome *2*. (**C**) Eye color phenotypes resulting from the expression of *mini-white* in the *P*-element inserted into the *Hr39* gene. The *A4* inversion leads to mosaic repression of *mini-white* in *A4/+*, *A4/A4*, *A12/A4*, and *A12/A4(ΔP)* flies. Dosage effect is seen in *A12/A12*, *A4/A4*, and *A12/A4* flies. (D) *trans*-Inactivation of the *mini-white* reporter (*P(w)*) on normal chromosome *2* in heterozygous *P(w)/A4(ΔP)* flies. The degree of *trans*-inactivation is ranked into four categories (+++, ++, +, −) according to the observed degree of *mini-white* repression. The examples of *trans*-inactivation phenotypes of four transgene insertions (*20708*, *20250*, *18735*, and *20102*) are shown. *P(w)/+* is a *mini-white* reporter over a wild-type chromosome; *P(w)/A4(ΔP)* is the same transgene over an *A4(ΔP)* chromosome.

AGO2 mutations $AGO2^{414}$ and $AGO2^{51B}$ (chromosome *3*) are viable and fertile in homozygous or *trans*-heterozygous states. Flies *P(w)/CyO*; *AGO2*/TM3*, *Sb Ser* and *A4/CyO*; *AGO2*/TM6U* were generated and crossed to get *P(w)/A4*; *AGO2*/AGO2** and *P(w)/A4*; *AGO2*/TM3*, *Sb Ser* (control) males.

To test the *Su(var)2-5* (*HP1a*) effect, the recombinant chromosome $Su(var)2\text{-}5^{01}$, *A4* was generated. Males w^{m4h}/Y; $Su(var)2\text{-}5^{01}/SM1$, *CyO* were crossed to females *yw/yw*; *A4/SM1*, *CyO*; then the F_1 females w^{m4h}/yw; *A4*/$Su(var)2\text{-}5^{01}$ were crossed to males *yw/Y*; *A4/SM1*, *CyO*. The F_2 recombinant females *yw/yw*; $Su(var)2\text{-}5^{01}$, *A4/SM1*, *CyO* were selected and crossed to males *yw/Y*; *P(w)/SM1*, *CyO*. Eye colors of *yw/Y*; $Su(var)2\text{-}5^{01}$, *A4/P(w)*, and *yw/Y*; *P(w)*/$Su(var)2\text{-}5^{01}$ males were compared.

RNA-Seq analysis

RNA samples were prepared from 2- to 3-day-old adult or third instar larval females of genotypes *A12/A12* and *A4/A4* reared at 18°. Homozygous nonfluorescent *A4/A4* female larvae were picked from the *A4/CyO-GFP* stock. Samples were prepared according to the standard Illumina protocol [TruSeq RNA Sample Prep Kit after rRNA depletion by Ribo-Zero rRNA Removal Kit (Human/Mouse/Rat), Epicentre] and sequenced on the Illumina HiSeq2000 (Laboratory of Evolutionary Genomics, Moscow State University). The following sequencing parameters were used: two biological replicas of each genotype and stage, single-end reading, read length 50 bp, and number of reads for each sample $\sim 2 \times 10^7$.

Raw reads were processed on a local Galaxy instance. The workflow included preprocessing of reads (FASTQ grooming, adapter removal, and quality trimming), transcript assembly, and gene-expression-level quantification by TopHat 0.6 and Cufflinks 0.0.7 using the dm3/R5 *Drosophila* gene set. The Cufflinks output tables with gene-level FPKM values (number of fragments per kilobase of assembled transcript per million fragments mapped to the transcriptome) were processed in

Excel. Genes with zero FPKM or with three times or more FPKM difference between replicates were removed, and the average FPKM values were used for $\log_2(A4/A12)$ calculation.

Next-generation sequencing (NGS) data are available under accession number GSE71842 at the NCBI Gene Expression Omnibus (GEO) website (http://www.ncbi.nlm.nih.gov/geo).

Messenger RNA (mRNA) quantification

mRNA abundances for the genes near the *A4* breakpoints were evaluated by real-time quantitative polymerase chain reaction (RT-qPCR). RNA was extracted from 2- to 3-day-old adult females or third instar female larvae *A12/A12* and *A4/A4* reared at 18° using the RNeasy Mini Kit (Qiagen). RNA was reverse transcribed with random hexamer primers. Evaluation of the normalized relative quantities (ΔΔCq) of transcripts was performed by real-time PCR using gene-specific primers and a DT-96 amplifier (DNA-Technology LLC). mRNA quantities in the samples were normalized to that of the housekeeping *RpL32* gene transcript. Log_2-transformed ratios of *A4* to *A12* transcript amounts were calculated from the three biological replicates. Average values and SDs are presented in the figures and in Table S3. The oligonucleotides used are listed in Table S2.

Chromatin immunoprecipitation (ChIP)

ChIP was performed as described previously (Klenov *et al.* 2007). Chromatin was extracted from third instar larvae and precipitated with antibodies against HP1a (Covance catalog #14923202) and H3K4me2 (Millipore #07-030). Two independent biological replicates were made. The enrichments were analyzed by RT-qPCR using a reference region 60D (chr2R:20322299–20322469) for sample quantity normalization. Primers used in ChIP measurements are listed in Table S2.

In situ hybridization and immunostaining

Mitotic chromosomes were prepared from *A4/A12* and *A12/A12* larval brains fixed according to Gatti *et al.* (1994) and mounted with a DAPI-containing medium (VECTASHIELD). Biotinylated oligonucleotides Biot-$(AACAC)_{10}$, Biot-$(GAGAA)_{10}$, and Biot-$(AATAACATAG)_5$ were used for *in situ* hybridization to reveal satellite DNA blocks on mitotic spreads. Mitotic chromosomes were stained with DAPI, and biotin signals were detected by Streptavidin, Alexa Fluor 546 (Life Technologies) under a fluorescent microscope.

Combined fluorescent immunostaining of proteins and DNA *in situ* hybridizations were performed according to a published protocol (Shpiz *et al.* 2014). Imaginal disks and salivary glands were isolated from the third instar larvae and hybridized to a biotinylated oligonucleotide probe for the AACAC satellite (chromosome *2* pericentromeric heterochromatin), a DIG-labeled probe for the 25-kb 39AB region (chr2L:21150645-21182675), and a Cy5-labeled probe for the histone gene cluster. The DIG-labeled probe for the 39AB region was generated by random priming of long-range PCR-amplified fragments from this region using DIG DNA Labeling Mix (Roche). The probe for the histone gene cluster was prepared by random priming of the PCR-amplified histone gene cluster unit (*His1* to *His3*) using a Cy5-labeled nucleotide. *In situ* hybridization was combined with polyclonal rabbit anti-HP1a staining (PRB-291C, Covance). Results of hybridization and immunostaining were visualized by Streptavidin, Alexa Fluor 546 (Life Technologies) for AACAC, anti-DIG-FITC AB (Roche) + anti-FITC Alexa 488 (Life Technologies) for the 39AB probe, and anti-rabbit–Alexa 514 conjugate (Life Technologies) for HP1a. The histone gene probe signal was detected by Cy5 fluorescence. Samples also were stained with DAPI to visualize nuclei. Oligonucleotides used for probe synthesis are listed in Table S2.

Samples were mounted in Slow Fade Medium (Invitrogen) for imaging in a Carl Zeiss LSM510 Meta Confocal Microscope equipped with a spectra analyzer and lasers of 405 (DAPI), 488 (FITC), 514, 546, and 633 nm. Three-dimensional (3D) images of stained nuclei were quantified in Imaris 7 software (Bitplane). The spots objects were generated in AACAC (histone gene cluster) 39AB probe *in situ* signal channels, and the mean intensity in the HP1a channel was calculated for each spot. The total number of treated nuclei was 100 for each genotype, and the average values and SDs for each *in situ* probe were calculated.

Software tools

We used local mirrors of the UCSC Genome Browser (https://genome.ucsc.edu) and Galaxy (https://usegalaxy.org) for data treatment and visualization. Custom tracks of the *A4* breakpoint position, positions of checked transgenes with color information representing sensitivity to *trans*-inactivation, and positions of probes for qPCR and *in situ* hybridization were created in BED (.bed) format, uploaded to the UCSC Genome Browser, and used for creation of the figures. Confocal image processing and calculations were done in Imaris 7.

Data availability

Created fly stocks are available upon request. Table S1 contains the list of fly lines bearing insertions used in the study. Stocks IDs are supplied. Table S2 contains the sequences of used primers. Table S3 contains treated NGS and qPCR data, Table S4 lists the alleles used in the study. Gene expression data are available at GEO with the accession number: GSE71842.

Results

Structure of A4 rearrangement

Inversion *A4* was produced by X-ray irradiation of the *A12* chromosome carrying a *mini-white*-containing *P*-element insertion. Irradiation caused two breakpoints, one in the 39B1 euchromatic section and the other in the pericentromeric

heterochromatin of chromosome *2*. The euchromatic breakpoint was localized to a 105-bp region (chr2L:21182214–21182318) of the second exon of the *Mcm10* gene using conventional genomic Southern blotting and PCR analysis (data not shown). The position of the heterochromatin breakpoint was revealed using differential staining of mitotic chromosomes from *A12/A4* individuals. The heterochromatic *h37* DAPI-bright region (Dimitri 1991) is split in *A4* into two parts, the larger part remaining at the centromere and the smaller part relocated to euchromatin (Figure 1, A and B). *In situ* fluorescence hybridization with several labeled satellite probes confirmed the cytologic localization of the heterochromatic breakpoint within the *h37* region containing the $(AATAACATAG)_n$ dodecasatellite (Lohe *et al.* 1993). Approximately one-third of the *h37* block is relocated to euchromatin.

A4 inversion results in two new euchromatin-heterochromatin borders—the border between euchromatin and a small, separated heterochromatin block (*h35–h37*) and the border between euchromatin and the main block of pericentromeric heterochromatin of chromosome *2*. Euchromatin sections 39B2–40F are inverted relative to normal chromosome orientation and placed between two heterochromatin blocks (Figure 1A).

Evaluation of cis-effects of heterochromatin in A4

The *A12* chromosome, the progenitor of the *A4* inversion, carries the *mini-white*-containing *P*-element in the 5′ UTR of the *Hr39* gene. Flies of genotype *A12/A12* have 10 times more eye pigment (quantitative data not shown) compared to *A12/+* flies, while the gene dosage increases just twice (Figure 1C). In the *A4* chromosome, the *mini-white* transgene is located 55 kb from the new euchromatin-heterochromatin border and demonstrates a strong variegated expression in both *A4/+* and *A4/A4* flies (Figure 1C). The eye color in *A4/A4* flies is significantly more intense than in *A4/+* flies, similar to the eye color difference between *A12/A12* and *A12/+* flies. The observed dosage effect of the expression of *mini-white* is specific to transgenes inserted at the beginning of the *Hr39* gene and is beyond the scope in this paper.

Variegated expression of the *mini-white* reporter in *A4/+* and *A4/A4* flies points to PEV caused by rearrangement. The effects of heterochromatin on neighboring euchromatic genes and the distance of inactivation spreading were evaluated using RNA-Seq analysis of the gene expression in *A4/A4* and *A12/A12* (control) larvae and adult females. qPCR verification of RNA-Seq data is presented for a set of genes scattered over a 500-kb region near the pericentromeric heterochromatin (39AE region) and a 50-kb region adjacent to the detached heterochromatic block (Figure 2 and Table S3). These regions in the normal chromosome demonstrate *trans*-inactivation of *mini-white* reporters when heterozygous with *A4* (see later). Thirty-four genes in the selected region have expression levels high enough for reliable quantification. The $\log_2$-transformed *A4/A4*-to-*A12/A12* ratio values for these genes are presented in Figure 2B.

In the region adjacent to the main (centromeric) heterochromatin, we found the only three genes showing a significant decrease (greater than twofold according to both RNA-Seq and qPCR) in mRNA abundance in *A4/A4* larvae compared to *A12/A12* larvae. These genes are located 35 kb (*CG8678* and *CG8679*) and 63 kb (*Hr39*) from the heterochromatin. In *A4/A4* adults, no decrease in *CG8679* and *Hr39* expression was observed, and a slightly increased expression of *CG8678* was detected. Surprisingly, the *CG8665* gene (189 kb from heterochromatin) demonstrated a strong fourfold activation at the larval stage in *A4/A4* larvae. In the region adjacent to the small, detached block of heterochromatin, we found a twofold increase in *Acon* gene expression in *A4/A4* larvae (13.5 kb from the breakpoint). No significant changes in gene expression in *A4/A4* compared to *A12/A12* flies were found at the adult stage.

Thus, analysis of gene expression at the euchromatin-heterochromatin border in *A4/A4* flies allows us to conclude that only a few genes respond to heterochromatin proximity, and their susceptibility to the effects of heterochromatin can vary at different developmental stages (*e.g.*, for the *CG8678* gene at the larval and adult stages) (Figure 2B). Some genes even demonstrate an increased expression, while the majority of euchromatic genes near the heterochromatin remain unaltered or demonstrate very small changes in expression.

We checked the chromatin state of the genes affected by PEV (*Acon*, *CG8678*, *CG8679*, *Hr39*, and *crc* as a negative control) by ChIP with anti-HP1a and anti-H3K4me2 antibodies. HP1a is a marker of heterochromatin, while the H3K4me2 histone modification associates with active transcription. Chromatin samples were prepared from *A12/A12* and *A4/A4* larvae, and the $\log_2$-transformed ratios of *A4/A4* to *A12/A12* enrichments in HP1a and H3K4me2 were calculated. Significant enrichments in HP1a (greater than twofold) were detected at the repressed *CG8679* and *Hr39* genes, while no changes occurred at the activated *Acon* or *crc* gene with an unchanged level of expression. A weak enrichment (1.5-fold) in HP1a was detected for the repressed *CG8678* gene. Changes in H3K4me2 were insignificant in all cases (Figure 2C). Thus, the increase in HP1a abundance underlies heterochromatin-caused *cis*-repression in tested genes.

Trans-Inactivation of mini-white reporters caused by A4 rearrangement

We noticed that *A12/A4* flies demonstrate variegated eye color (Figure 1C), while *A12/A12* or *A12/+* flies have uniformly colored eyes. The same variegated phenotype is observed in *A12/A4(ΔP)* flies carrying the inversion lacking the *mini-white* transgene (Figure 1C). This observation points to the ability of the *A4* inversion to inactivate genes on the homologous normal chromosome (*trans*-inactivation). To evaluate the area of *trans*-inactivation, we checked 69 *mini-white*-containing transgenes (see *Materials and Methods* and Table S1) scattered throughout the 38D–40F region for their susceptibility to *trans*-inactivation by the *A4* rearrangement.

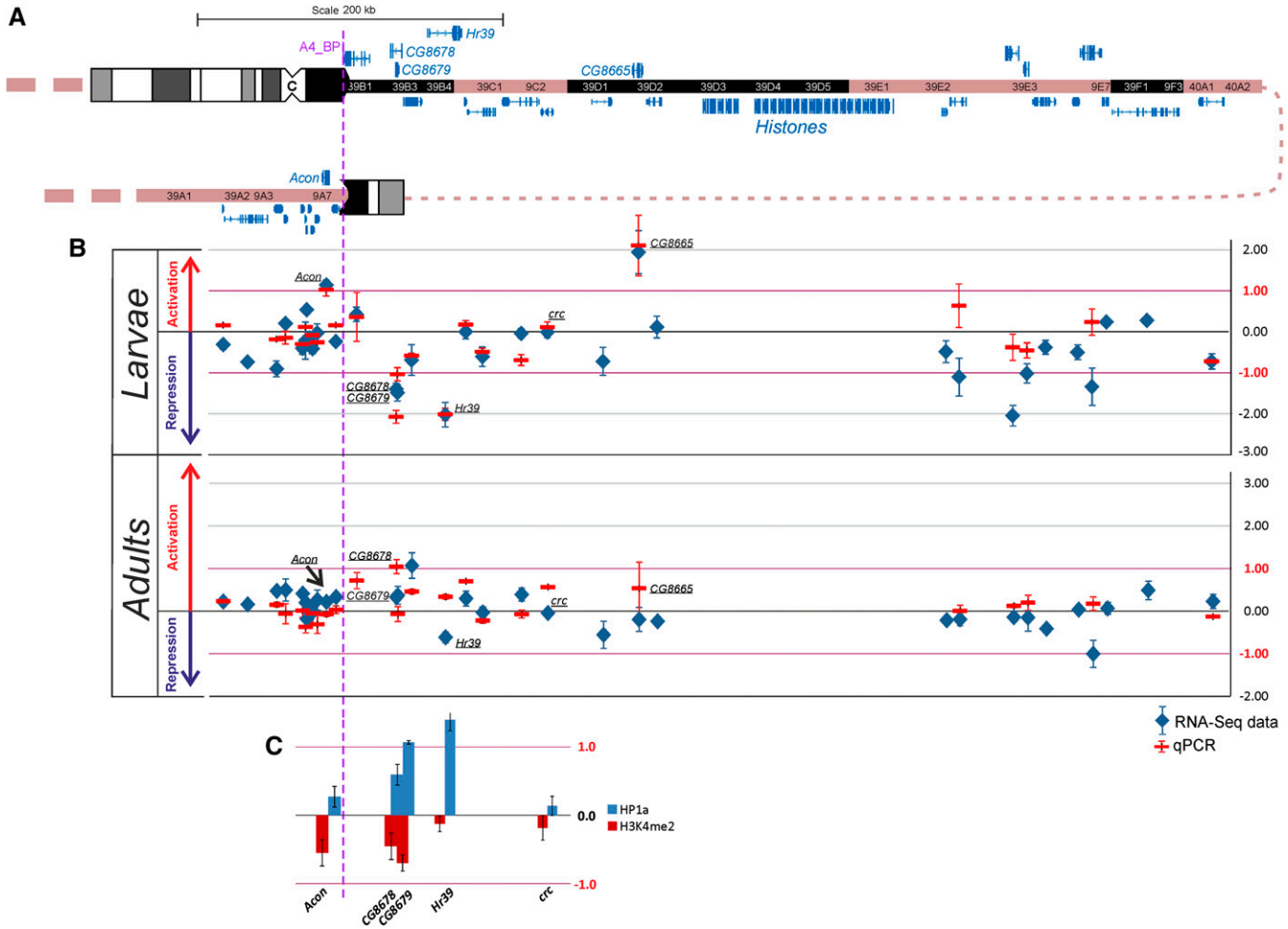

Figure 2 *cis*-Effects of heterochromatin in the *A4* inversion in larvae and adults. (A) Structure of the *A4* inversion. C, centromere. Black, gray, and white blocks represent the organization of heterochromatin of chromosome *2* (Dimitri 1991). Exon-intron maps of the genes in the region are presented, and the genes with confirmed greater than twofold expression changes in either larvae or adults have captions. Euchromatic position of the *A4* breakpoint is shown by the vertical dotted line. (B) Chromosome distributions of $\log_2$-transformed ratios (*A4*/*A4* to *A12*/*A12*) of normalized gene expression levels based on RNA-Seq (blue diamonds) and qPCR (horizontal red strips) data. *cis*-Repression corresponds to negative values. These data show that euchromatic genes respond to heterochromatin-induced *cis*-effects individually and differently in larvae and adults. (C) Changes in HP1a and H3K4me2 abundance ($\log_2$-transformed *A4*/*A4*-to-*A12*/*A12* ratio) for the genes *Acon*, *CG8678*, *CG8679*, *Hr39*, and *crc* at the larval stage. The positions of the bars correspond to the positions of genes on the chromosome. Genes *Acon*, *CG8678*, *CG8679*, *Hr39*, but not *crc* change their expression near the heterochromatin (B). Significant changes (greater than twofold) in HP1a are detected for the *Hr39* and *CG8678* genes, and no significant difference is observed for H3K4me2 enrichments.

These transgenes are located in the 1.5-Mb region (38D–40F) around the position corresponding to the euchromatic breakpoint in *A4*.

A4 induces *trans*-inactivation of the *mini-white* reporters, and the *trans*-inactivation exhibits uneven distribution over a wide area starting from the position of the euchromatic breakpoint in *A4*. Two distinct areas of *trans*-inactivation were detected; the first, smaller one is homologous to the euchromatic region adjacent to the separated small heterochromatin block in *A4* (Figure 3, region A), and the second, much more extended one corresponds to the euchromatic part of chromosome *2L* transposed to pericentromeric heterochromatin in *A4* (Figure 3, regions B, C, and E). *trans*-Inactivation in region A spreads over a distance of approximately 40 kb, while the second area encompasses 476 kb because inactivation of the *19883* transgene located in the 39E3 region is detectable (Figure 3, region E, bold). An irregular pattern of *mini-white trans*-inactivation was found in the second area. Continuous repression is observed in the 40-kb region adjacent to the centromeric heterochromatin (region B), which is followed by the 80-kb region of interspersed inactivation (region C), where some transgenes are turned off and others are active. No *trans*-inactivation was detected near the histone gene cluster (region D), but we found an ~45-kb "island" of *trans*-inactivation after the histone gene cluster (region E).

A4 inversion induces repression of *mini-white* reporters on the homologous normal chromosome. In the region near the euchromatin-heterochromatin border (~40 kb in size), transgenes of any tested type in any position could be

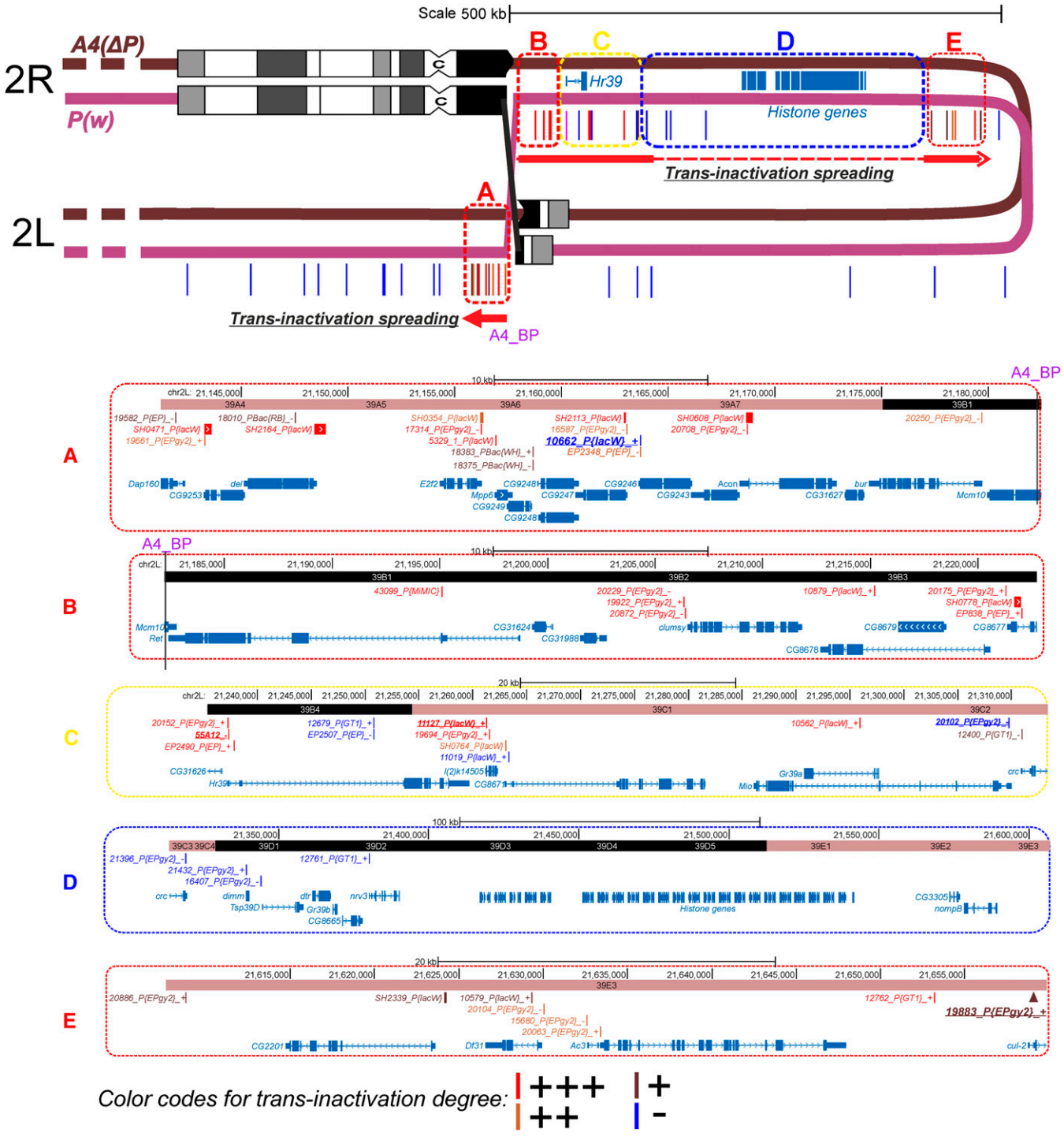

Figure 3 Detailed map of *mini-white* reporter *trans*-inactivation in *A4(ΔP)/P(w)* flies. (Top) Schematic representation of paired *A4(ΔP)* and transgene-bearing *P(w)* chromosomes forming an inversion loop. The *A4(ΔP)* chromosome contains pericentromeric and detached smaller heterochromatin blocks that cause propagations of *trans*-inactivation (shown by thick red arrows). Colored vertical strokes represent the positions and degree of transgene repression: red, strong inactivation; orange, moderate inactivation; brown, weak inactivation; and blue, no inactivation. The whole area of *trans*-inactivation spreading is subdivided into regions of total repression (A and B with the single exception of *10662*), moderate/interspersed repression (C and E), and no repression (D) of inserted transgenes. Dashed colored lines outline the approximate borders of these regions. (Bottom) Close-up views of regions A, B, C, D, and E showing the positions of endogenous genes and transgene insertions. Transgene names are constructed as "stock number_transgene type_insertion orientation"; the colors of transgenes correspond to the degree of repression, as in the top panel. Regions A and B, ~40 kb each, are immediately adjacent to heterochromatin in the *A4* chromosome. Region C is the region of interspersed inactivation (~80 kb). Region D includes the histone gene cluster; no *trans*-inactivation is observed here. Region E is the "island" of *trans*-inactivation after the histone gene cluster. The furthermost transgene still repressed is *19883* (region E, 475 kb from the breakpoint position).

trans-inactivated, in contrast to *cis*-repression of euchromatic genes near the *A4* breakpoint.

HP1a occupancies at the trans-inactivated transgene are independent of chromatin state at homologous sites on the A4 chromosome

A comparison of *cis*-effects of heterochromatin on a given gene in *A4* and *trans*-inactivation of the transgene inserted into this gene on the homologous chromosome reveals no correlation between the two effects. For instance, the *Acon* gene demonstrates *cis*-activation in *A4/A4* larvae, while the *20708* insertion in its 5′ UTR is strongly *trans*-inactivated (Figure 2 and Figure 3). We suggest that the formation of repressive chromatin in the transgene occurs independently of the chromatin state of the homologous region on *A4*. To check this assumption directly, we compared HP1a enrichments inside the transgenes and at the sites of transgene insertion on the *A4(ΔP)* chromosome by ChIP.

We checked the chromatin state of the two transgenes, *trans*-inactivated *11127* (*P[lacW]* in *l(2)k14505*) and noninactivated *20102* (*P[EPgy2]* in *Mio*). Samples were prepared from the *w**; *11127/A4(ΔP)*, *w**; *20102/A4(ΔP)*, and *w**; *11127/+*, *w**; *20102/+* (control) third instar larvae because *mini-white* expression starts at this developmental stage, and the most prominent effects of heterochromatin on gene expression were observed in the larvae based on RNA-Seq data.

Figure 4 presents the design of the experiment, including the positions of the primers used. Primers to *mini-white* and *LacZ* genes were applied for HP1a and H3K4me2 enrichment measurements in insertion *11127*. There is no *LacZ* in insertion *20102*; just primers to *mini-white* were used in this case. To measure the occupancies of HP1a and H3K4me2 at the sites on the *A4(ΔP)* chromosome corresponding to the place of *11127* transgene insertion, we used a primer pair designated as 11127. The PCR product from this primer pair overlaps the place of insertion of the respective transgene (Figure 4).

We found more than a twofold enrichment in HP1a at the *mini-white* and *LacZ* genes in *trans*-inactivated transgene *11127* (in *11127/A4(ΔP)* relative to the *11127/+* control). The changes in the H3K4me2 modification level were insignificant, with a tendency to drop at *LacZ* (Figure 4B, lower histogram). No significant enrichments of HP1a or H3K4me2 were detected at the *mini-white* gene of noninactivated transgene *20102* (in *20102/A4(ΔP)* relative to the *20102/+* control) (Figure 4C, lower histogram).

The site opposite the *11127* transgene on the *A4(ΔP)* chromosome showed no significant enrichments in HP1a in the absence of this transgene (in *20102/A4(ΔP)* relative to the *20102/+* control) (Figure 4C, top histogram). However, in the presence of the transgene (in *11127/A4(ΔP)* larvae), HP1a enrichment was detected on the *A4(ΔP)* chromosome in the place of the *11127* transgene insertion (Figure 4B, top histogram). Since the HP1a accumulates at the *11127* in *11127/A4(ΔP)* (as mentioned earlier), we suggest that the heterochromatinization of the transgene occurs *de novo* and is not caused by HP1a spreading from neighboring regions. The heterochromatinization of the *trans*-inactivated transgene probably induces the accumulation of HP1a on the opposite site on the homologous chromosome. Results of ChIP experiments demonstrate that the *trans*-inactivated transgene binds HP1a and that autonomous heterochromatinization of the transgene could induce the accumulation of HP1a on the opposite chromosome.

Trans-Inactivation and the nuclear position of the histone cluster

The small, detached heterochromatin block in the *A4* chromosome tends to conjugate with the pericentromeric heterochromatin in *A4/A4* flies and is able to drag regions of somatically paired normal chromosome (in *A4/+* flies) into the heterochromatic nuclear compartment (Abramov *et al.* 2011; Lavrov *et al.* 2013; unpublished data). Inversion *A4* produces a peculiar pattern of *mini-white* transgene *trans*-inactivation along the chromosome: repression occurs on both sides of the histone gene cluster, while several transgenes (*21396*, *21432*, *16407*, and *12761*) (Figure 3, region D) located close to the cluster show no *mini-white* repression. To check the correlation of this effect with a specific nuclear compartmentalization of the histone gene cluster, we performed combined *in situ* hybridization and HP1a immunostaining of nuclei from *A12/A12* and *A12/A4* larval imaginal disks. The heterochromatic compartment was detected by HP1a staining, and the intranuclear positions of chromosome regions were visualized using DNA probes for the 39AB region (35-kb fragment immediately adjacent to the euchromatic breakpoint), the histone gene cluster, and the AACAC satellite as a marker of pericentromeric heterochromatin of chromosome *2*. One hundred interphase nuclei of both genotypes were analyzed using a confocal microscope.

The number of signals for each hybridization probe per nuclei and the position of each probe relative to an HP1a-stained subvolume of nuclei volume were estimated. Single spots for the 39AB region and the histone gene cluster were revealed in 92% of *A4/A12* nuclei and 94% of *A12/A12* nuclei. These data indicate the essentially complete pairing of homologs both in the case of normal chromosomes (*A12/A12*) and in *trans*-heterozygous combinations of normal and rearranged chromosomes (*A4/A12*).

We found that the histone gene cluster localizes in both *A4/A12* and *A12/A12* nuclei at the border of the highly enriched HP1a area (97% of nuclei). The 39AB fragment, representing the *trans*-inactivated area, locates in the euchromatin in *A12/A12* nuclei, while in *A12/A4* nuclei it is detectable inside the HP1a-stained compartment (Figure 5). To confirm this observation, measurements of the mean intensities of HP1a staining at the positions of *in situ* hybridization signals of the AACAC satellite, the histone gene cluster, and the 39AB region were performed (described in *Materials and Methods*). The measurements show that the concentration of

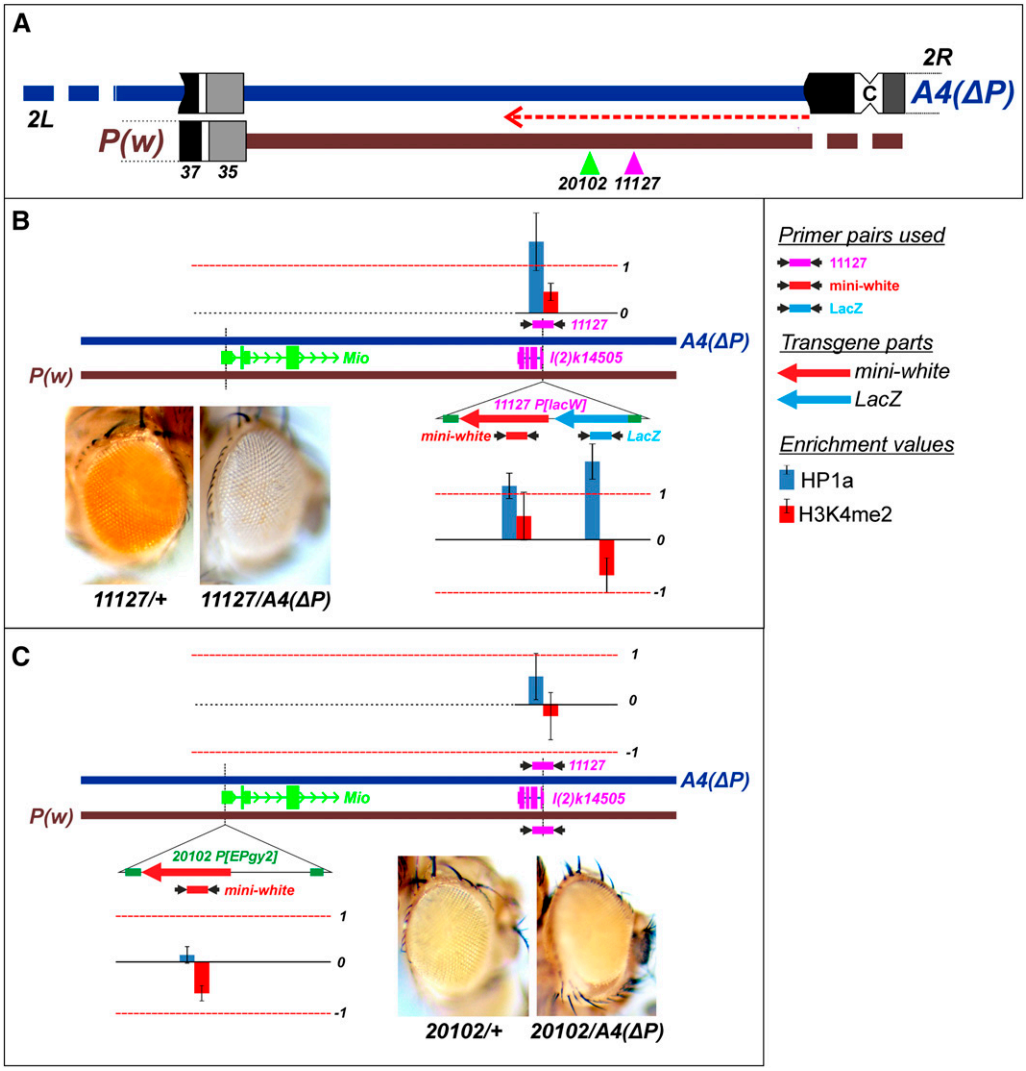

Figure 4 HP1a accumulates at the *trans*-inactivated transgene and on *A4* at the site homologous to insertion of the *trans*-inactivated reporter. Primer pairs used for ChIP analysis of the transgenes (*mini-white*, *LacZ*) and the site on the *A4(ΔP)* chromosome corresponding to transgene insertion *11127* are marked by different colors. The histogram bars in B and C presents the $\log_2$-transformed ratios of HP1a (blue) or H3K4me2 (red) abundance in *P(w)/A4(ΔP)* individuals to *P(w)/+* individuals; the bar positions correspond to the locations of the regions analyzed. The *trans*-inactivation phenotypes are shown for *11127* and *20102*. (A) Fragments of *A4(ΔP)* inversion and normal *P(w)* chromosome carrying reporter transgenes. The direction of *trans*-inactivation spreading along the nonrearranged chromosome is indicated by the red dotted arrow. The positions of the *11127* (*trans*-inactivated) and *20102* (noninactivated) transgenes are indicated by pink and green triangles, respectively. (B) *trans*-Inactivated insertion *11127* in *11127/A4(ΔP)* larvae. The scheme shows the arrangement of the *11127* and *A4(ΔP)* chromosomes, positions of insertion and primers, and the simplified structure of the *P[lacW]* transgene inserted (below the chromosome). The positions of histogram bars showing the HP1a and H3K4me2 enrichment levels correspond to the positions of primers. HP1a accumulates at the constituents of *trans*-inactivated transgene *11127* (histogram below the transgene image) and in the site of this transgene insertion on the opposite *A4(ΔP)* chromosome (primers 11127). (C) Noninactivated insertion *20102* in *20102/A4(ΔP)* larvae (for designations, see B). No accumulation of HP1a in the *mini-white* of transgene *20102* was observed. There was also no accumulation of HP1a in the site of transgene *11127* insertion in the absence of the proper transgene. A significant enrichment in HP1a was observed in *trans*-inactivated but not in noninactivated transgenes. The comparison of chromatin state on *A4(ΔP)* when heterozygous with the *trans*-inactivated transgene reveals an HP1a enrichment.

HP1a at the position of 39AB is higher in *A4/A12* nuclei than in *A12/A12* nuclei and that the concentration of HP1a in the position of the histone gene cluster remains approximately the same in *A4/A12* and *A12/A12* nuclei but is lower than at the position of the AACAC satellite (Figure 5C).

The 39AB probe, which corresponds to region A of continuous *trans*-inactivation (Figure 3), produces a single hybridization spot in most *A4/A12* nuclei. Region A is normally (in *A12/A12* nuclei) located in euchromatin and is dragged into the HP1a-rich compartment in *A4/A12* nuclei. The probe for the histone gene cluster corresponds to region D, where no *trans*-inactivation is observed (Figure 3). Despite the conjugation of *A4* with *A12*, the histone gene cluster tends to be excluded from the heterochromatic compartment to the border of the HP1a-enriched area. We assume that the histone gene cluster stays out of the heterochromatic compartment, thus suppressing *trans*-inactivation in its vicinity.

Genetic modifiers of trans-inactivation

We tested several well-known modifiers of PEV for their ability to affect *trans*-inactivation (see *Materials and Methods* and Table S4). The eye phenotypes in Figure 6 are presented for transgene *11127*, located in region D with interspersed *trans*-inactivation (Figure 3).

Most traditional PEV modifier mutations tested (*i.e.*, *Su(var)2-5*, *Su(var)3-1*, *Su(var)3-6*, and *Su(var)3-7*) suppress *trans*-inactivation of transgenes and *cis*-inactivation of the reporter *mini-white* inserted in the *Hr39* gene in *A4* (Table S4). The exception is the mutations in the *Su(var)3-9* gene, which have no effect on *trans*- or *cis*-inactivation of *mini-white* in the *A4*

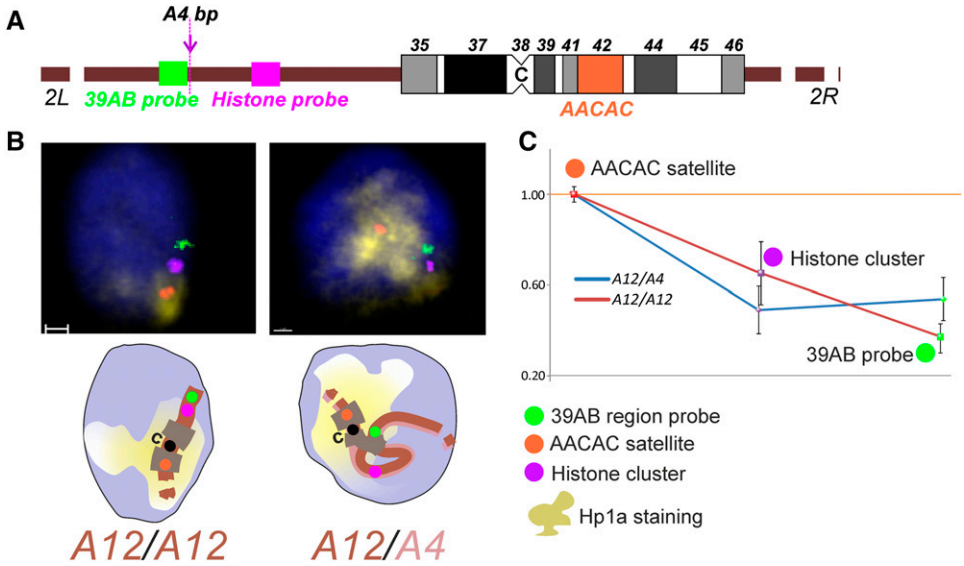

Figure 5 The 39AB region located in *A12/A12* nuclei in euchromatin is moved to the heterochromatic compartment in *A12/A4*, while the histone gene cluster maintains its position at the euchromatin-heterochromatic border. (A) The positions of the *in situ* probes for 39AB (green), histone gene cluster (pink), and AACAC satellite (red) are shown on a schematic chromosome *2* map. The arrow points to the position of the *A4* breakpoint. (B) Examples of confocal nuclei cross section and the schematic view (below) of paired homologous chromosomes of typical *A12/A12* and *A12/A4* nuclei after *in situ* staining. C, centromere. Colored dots on the scheme represent the positions of the *in situ* hybridization probes; their colors correspond to those of the FISH signals on the confocal images and on the chromosome scheme at the top. The yellow cloud is HP1a staining of the heterochromatin compartment. (C) Mean HP1a staining intensities calculated at the positions of *in situ* signals of the histone gene cluster and the 39AB region and normalized to the mean intensity of HP1a staining at the position of the AACAC satellite signal.

chromosome. The *Su(var)3-9* gene encodes histone methyltransferase, one of the key components of the heterochromatin-spreading mechanism (Schotta *et al.* 2002). However, mutation in the *eggless* gene encoding another histone methyltransferase, SETDB1, strongly suppresses *trans*-inactivation of transgenes as well as *cis*-inactivation of *mini-white* in *A4* (not shown).

We detected opposite effects on *trans*-inactivation of two proteins known to be involved in chromatin state maintenance. *trans*-Inactivation but not *cis*-inactivation of *mini-white* in *A4* is strongly suppressed by the $e(y)3^{u1}$ mutation affecting the supporter of activation of yellow protein [SAYP, a coactivator/subunit of the Brahma remodeling complex (Chalkley *et al.* 2008) and an essential component for heterochromatin establishment on chromosome *4* (Shidlovskii *et al.* 2005)]. We also found that the AGO2 protein acts as a potent suppressor of *trans*-inactivation. This protein was earlier described as a component of the insulator complex (Moshkovich *et al.* 2011), and loss of its function disturbed transcription in *Drosophila* (Cernilogar *et al.* 2011). Homozygous (*P(w)/A4*; $AGO2^{414}/AGO2^{414}$) or *trans*-heterozygous (*P(w)/A4*; $AGO2^{414}/AGO2^{51B}$) males have white eyes, contrary to their heterozygous siblings, with colored eyes (Figure 6). *AGO2* mutations also exert a smaller but discernible enhancer effect on *cis*-inactivation in *A4*.

Mutations in genes *UAP56* (a component of mRNA nuclear transport), *zeste* (which affects transvection), and *piwi* (a component of the PIWI-interacting RNA silencing pathway) have no effect on *trans*-inactivation (not shown), although they have been reported as PEV or chromosomal interaction modifiers (Hazelrigg and Petersen 1992; Eberl *et al.* 1997; Pal-Bhadra *et al.* 2004).

Discussion

In this paper, we describe the genetic system inversion *A4* in chromosome *2*, which provides an opportunity to explore simultaneously the *cis*- and *trans*-effects of a euchromatin-heterochromatic rearrangement. This inversion was originated by irradiation-induced breakpoints in euchromatin and in the block of dodecasatellite in pericentromeric heterochromatin of the normal progenitor *A12* chromosome carrying the *mini-white* reporter. *A4* causes a variegated phenotype of the *mini-white* reporter located 55 kb from the border with the main centromeric heterochromatin block. *A4* also causes *trans*-inactivation of the *mini-white*-containing transgenes located on the nonrearranged chromosome in regions homologous to those adjacent to heterochromatin in *A4* (Figure 1 and Figure 3).

To check the degree of propagation of heterochromatin *cis*-acting effects, we measured the expression levels of genes in *A4/A4* and *A12/A12* adult and third instar female flies (Figure 2 and Table S3). To our knowledge, this is the first PEV study using RNA-Seq profiling. We found that most euchromatic genes in their natural environment (contrary to reporter transgenes) are resistant to the influence of heterochromatin in the *A4* inversion. A significant decrease in mRNA level was shown only for 3 genes (*G8678*, *CG8679*, and *Hr39*) of 34 analyzed genes in *A4* larvae, and no significant changes in expression were detected in adults. Our observation that the expression of most heterochromatin-relocated genes is unaltered is similar to the results of an earlier study of *white-mottled* inversions (Vogel *et al.* 2009). These authors demonstrated a notable decrease in the expression of only the *white* gene of 20 tested genes relocated to heterochromatin. The authors suggested that the *white* gene has an unusual intrinsic affinity for heterochromatin, which may render this gene more susceptible to silencing by heterochromatin than most other genes.

Obviously, the *white* gene is not the unique target of PEV. There are a number of examples of PEV of different genes in classical genetics studies (Spofford 1976). In the case of *A4*

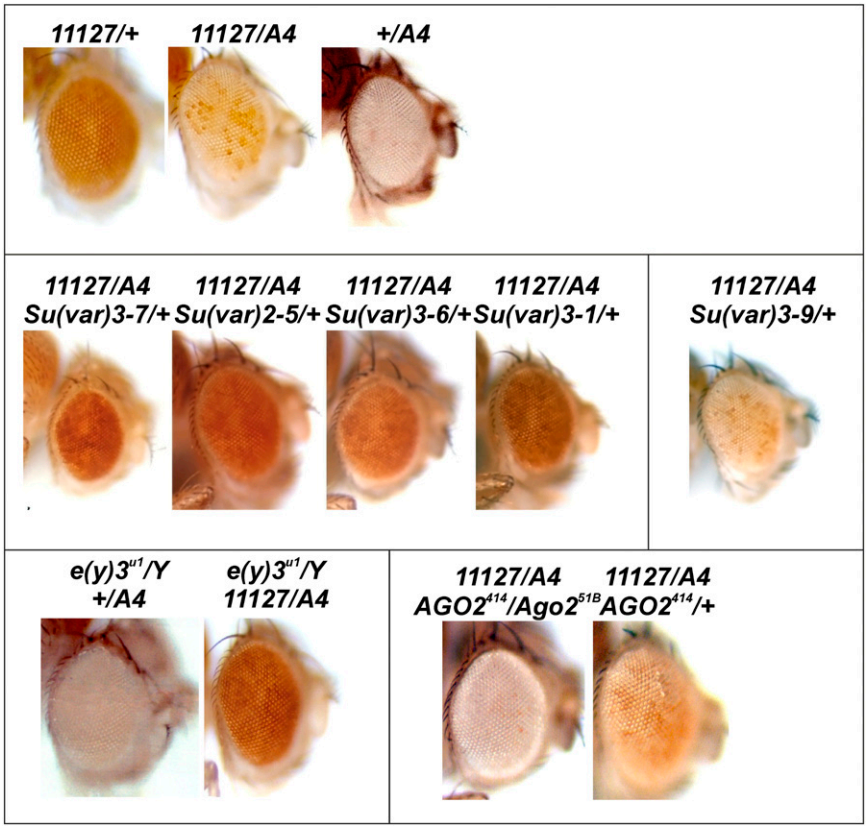

Figure 6 Effect of PEV modifiers and the *e(y)3* transcriptional coactivator on *trans*-inactivation. *trans*-Inactivated transgene *11127* is the insertion of *P[lacW]* at a distance of 80 kb from the border between euchromatin and the pericentromeric block of heterochromatin in *A4*. *Su(var)2-5*, *Su(var)3-7*, *Su(var)3-6*, and *Su(var)3-1* suppress *trans*-inactivation of *mini-white* in *11127/A4* flies. *Su(var)3-9* does not suppress *trans*-inactivation, while $e(y)3^{u1}$ suppresses *trans*- but not *cis*-inactivation. *AGO2* mutations ($AGO2^{414}/AGO2^{51B}$ and $AGO2^{414}/AGO2^{414}$ have the same effect) enhance *trans*-inactivation but to a much lesser degree *cis*-inactivation of *mini-white* in *A4*.

rearrangement, three different genes are repressed in heterochromatin proximity. The features making a gene amenable to heterochromatin repression are not known at present, but one possibility could be ruled out in our study. There is no visible correlation between the transcription level of the gene and the degree of repression under the influence of heterochromatin. This follows from a comparison of expression levels of genes in the RNA-Seq data (Table S5).

Surprisingly, we showed not only repression but also activation of two genes located near the heterochromatin in the region visibly heterochromatinized in the *A4* polytene chromosomes (data not shown). Expression of the *Acon* gene (evaluated by both RT-qPCR and RNA-Seq) increased twofold and expression of the *CG8665* gene increased fourfold in *A4/A4* larvae compared to individuals carrying the progenitor nonrearranged chromosome *A12*. The detected cases of gene upregulation in *A4* could be explained by taking into account the reported ability of HP1a not only to repress but also to activate individual genes (Cryderman *et al.* 2005; De Lucia *et al.* 2005; Hediger and Gasser 2006; de Wit *et al.* 2007; Cryderman *et al.* 2011; Eissenberg and Elgin 2014).

We found that the heterochromatin effect on a given gene in *A4* depends on the developmental stage because all the genes demonstrating repression or activation in third instar larvae showed no significant expression changes in adults. This observation may be explained by assuming that the heterochromatinization perturbs not the transcription itself but the changes in gene transcription state (either activation or repression), which are, in turn, coupled with chromatin remodeling. The late larval stage is the period when a vast number of genes change their transcription state and presumably become sensitive to heterochromatin influence.

The *A4* inversion is able to induce *trans*-inactivation of reporter transgenes on the homologous chromosome. This ability was shown primarily by the observation of variegated eye phenotype in *A12/A4* flies (Figure 1C). *trans*-Inactivation caused by *A4* was probed using the *mini-white*-containing transgenes located on the normal chromosome *2* in the regions that are homologous to the *A4* regions adjacent to heterochromatin. *trans*-Inactivation spreads over an area of 475 kb from the main satellite block (up to transgene *19883*) (Figure 3, region E) and over an area of 40 kb (Figure 3, region A) from the small, detached heterochromatic block.

Inactivation of transgenes on the normal chromosome in combination with *A4* is continuous both in the 40-kb area adjacent to the main block of pericentromeric heterochromatin and near the small, detached heterochromatic block (Figure 3, regions A and B). All types of transgenes inserted into promoters and coding and intergenic regions undergo inactivation. The single exception in this region is the noninactivated *10662* (*P[lacW]*) transgene inserted into the 5′ UTR of the *CG9246* gene 18.6 kb from the small, detached block of heterochromatin. The presence of a GAGA factor binding site in *P[EP]* and *P[EPgy2]* transgenes or the *Su(Hw)* binding site in *PBac[WH]* genes does not prevent repression. These sites demonstrate insulator properties, but it seems that two

copies should flank the reporter gene to obtain effective protection from inactivation.

The region ~80 kb in size (Figure 3, region C) demonstrates interspersed *trans*-inactivation. Closely located transgene pairs with different responses to inactivation are represented by *SH0764* (*P[lacW]*)*/11019* (*P[lacW]*) and *20102* (*P[EPgy2]*)*/12400* (*P[GT1]*). The first pair lies in the 5′ UTR of the *CG8671* gene, and the insertions are separated by 326 bp. Transgene *SH0764* but not *11019* is sensitive to *trans*-inactivation, and both are of the same type, *P[lacW]*. In the second pair of transgenes separated by 500 bp, *20102* is not *trans*-inactivated, while *12400* is moderately inactivated. Transgene *20102* is inserted upstream of the *crc* gene, and *12400* is in its 5′ UTR.

We revealed different responses to *trans*-inactivation of transgenes separated by only 9 bp (*10662* and *EP2348* in the 5′ UTR of the *CG9246* gene) (Figure 3, region A), which raises the question of whether chromatin organization at the insertion site is a determining factor of *trans*-inactivation. Rather, the differences in *trans*-inactivation of closely located transgenes can be explained by the formation of individual chromatin structures including functional elements of the transgene and its target in each case of insertion.

The effects of *cis*- and *trans*-inactivation of heterochromatin on the homologous regions on the rearranged and normal chromosomes do not follow each other (Figure 2 and Figure 3). Euchromatic genes in their natural environment appear to be quite resistant to heterochromatin influence, presumably because of the presence of full sets of regulatory elements (*i.e.*, enhancers, insulators, etc.). Just a few genes near the euchromatin-heterochromatin border in the *A4* chromosome are affected, while the inactivation of transgenes on the homologous chromosome is strong and can be detected far from heterochromatin. Transgenes containing *mini-white* reporters are quite sensitive to repression when placed into a heterochromatin environment [this work, the bw^D example, and earlier observations such as those of Martin-Morris *et al.* (1997)], presumably because of the lack of a full set of regulatory elements.

Transgenes in the same region (*e.g.*, the abovementioned *11127* and *20102*) (Figure 3, region C) can be inactivated or not, respectively, and we suppose that heterochromatin formation proceeds autonomously on a transgene dragged into the heterochromatic compartment and may induce heterochromatinization on the homologous rearranged chromosome, an initiator of the dragging of the heterochromatic compartment, and subsequent *trans*-inactivation (Figure 4).

An additional observation pointing to different mechanisms of *cis*- and *trans*-inactivation is the existence of mutations specifically affecting *trans*- but not *cis*-inactivation in *A4*. We showed that two chromatin-related proteins, SAYP and AGO2, act as potent noncanonic PEV modifiers of *trans*-inactivation. SAYP protein, a subunit of the *SWI/SNF* complex (Chalkley *et al.* 2008) has been characterized as a chromatin coactivator (Shidlovskii *et al.* 2005). At the same time, SAYP binds to heterochromatin, and its deficiency suppresses heterochromatin-induced repression of transgenes and the *white* gene in the w^{m4h} inversion (Shidlovskii *et al.* 2005). In our case, *SAYP* mutation strongly suppresses *trans*-inactivation but not *cis*-repression of transgenes in *A4* (Figure 6). *AGO2* mutations, by contrast, enhance *trans*-inactivation but just slightly affect *cis*-repression of transgene in *A4* (Figure 6). Apart from its role in siRNA-based RNA interference (RNAi), AGO2 is considered to be a component of active chromatin in *Drosophila* (Cernilogar *et al.* 2011) and an insulator-associated protein (Cernilogar *et al.* 2011; Moshkovich *et al.* 2011). Although the exact mechanisms of the opposite effects of *AGO2* and *SAYP* mutations on *trans*-inactivation remain obscure, it is possible that SAYP directly participates in the heterochromatinization *de novo*, while AGO2 is necessary for the proper functioning of insulators around the *trans*-inactivated reporter gene.

trans-Inactivation caused by *A4* shows similarities to the earlier-studied ability of the bw^D allele to silence the homologous *bw* allele and the *mini-white*-containing transgenes *in trans*. Up to the present, bw^D was essentially unique and the most extensively explored example of PEV-induced *trans*-inactivation in the fruit fly. bw^D was caused by insertion of the AAGAG satellite (1.6 Mb) into the coding sequence of the *brown* gene (Sage *et al.* 2005). It was expected and then experimentally confirmed that the presence of somatic pairing of the homologous chromosome in *Drosophila* and the ability of heterochromatic repeated regions to stick together underlie the dragging of euchromatin into the heterochromatic compartment by the bw^D allele (Csink and Henikoff 1996, 1998; Fung *et al.* 1998; Thakar and Csink 2005). The molecular mechanism of heterochromatin formation in *trans*-inactivation differs from its *cis*-spreading because it is independent of the histone methyltransferase SU(VAR)3-9 (Nisha *et al.* 2008). In the case of bw^D *trans*-inactivation, deletion mapping (Sage *et al.* 2005) identified the 301-bp region acting as an enhancer of *trans*-inactivation; it contained multiple binding sites for BEAF insulator protein and was enriched by BEAF (according to the ChIP chip profile modENCODE). However, we found no obvious correlations between BEAF enrichment and transgene inactivation sites using the modENCODE BEAF profile.

We found no *trans*-inactivation of transgenes in the region immediately proximal to the histone gene cluster (Figure 3, region D), while it occurred further away from both sides of the cluster. Since *A4*, like bw^D, causes dragging of euchromatic regions into the heterochromatic compartment (Abramov *et al.* 2011; Lavrov *et al.* 2013), we checked whether a distinct intranuclear placement of the histone gene cluster may be responsible for the suppression of *trans*-inactivation. 3D confocal imaging using probes for the *trans*-inactivated region and the histone gene cluster shows that the latter forms a distinct subcompartment located on the border of the heterochromatic compartment but outside of it (Figure 5). We assume that this is the reason for the large-scale gap in *trans*-inactivation spreading near the histone gene cluster.

Studies of the genetic system described herein allow us to consider *cis*- and *trans*-inactivation driven by chromosomal rearrangement as two relatively independent processes of heterochromatinization. We showed no correlation between *cis*-repression of genes near the euchromatin-heterochromatin border and inactivation of transgenes on a homologous chromosome (Figure 2 and Figure 3). The process of transgene heterochromatinization seems to be independent of *cis*-spreading of heterochromatin because the binding of HP1a to the transgene occurs in the absence of HP1a at the homologous site on the rearranged *A4* chromosome. The detection of genes specifically affecting the *trans*-inactivation process also points to different mechanisms of *cis*-repression and transgene inactivation.

Acknowledgments

We are grateful to M. Logacheva (A. Kondrashov Group at Moscow State University) for performing NGS runs and to Yu. Shevelyov for helpful discussion. Stocks obtained from the Bloomington Drosophila Stock Center (National Institutes of Health P40-OD018537) were used in this study. This work was supported by grants from the Russian Foundation for Basic Research (13-04-40138 to V.A.G. and 14-04-32308 to A.S.Sh.) and the Molecular and Cell Biology Program of the Russian Academy of Sciences (to V.A.G).

Literature Cited

Abramov, Y. A., M. V. Kibanov, V. A. Gvozdev, and S. A. Lavrov, 2011 Genetic and molecular analysis of gene trans-inactivation caused by homologous eu-heterochromatic chromosome rearrangement in Drosophila melanogaster. Dokl. Biochem. Biophys. 437: 72–76.

Cernilogar, F. M., M. C. Onorati, G. O. Kothe, A. M. Burroughs, K. M. Parsi *et al.*, 2011 Chromatin-associated RNA interference components contribute to transcriptional regulation in Drosophila. Nature 480: 391–395.

Chalkley, G. E., Y. M. Moshkin, K. Langenberg, K. Bezstarosti, A. Blastyak *et al.*, 2008 The transcriptional coactivator SAYP is a trithorax group signature subunit of the PBAP chromatin remodeling complex. Mol. Cell. Biol. 28: 2920–2929.

Cryderman, D. E., S. K. Grade, Y. Li, L. Fanti, S. Pimpinelli *et al.*, 2005 Role of Drosophila HP1 in euchromatic gene expression. Dev. Dyn. 232: 767–774.

Cryderman, D. E., M. W. Vitalini, and L. L. Wallrath, 2011 Heterochromatin protein 1a is required for an open chromatin structure. Transcription 2: 95–99.

Csink, A. K., and S. Henikoff, 1996 Genetic modification of heterochromatic association and nuclear organization in Drosophila. Nature 381: 529–531.

Csink, A. K., and S. Henikoff, 1998 Large-scale chromosomal movements during interphase progression in Drosophila. J. Cell Biol. 143: 13–22.

De Lucia, F., J. Q. Ni, C. Vaillant, and F. L. Sun, 2005 HP1 modulates the transcription of cell-cycle regulators in Drosophila melanogaster. Nucleic Acids Res. 33: 2852–2858.

de Wit, E., F. Greil, and B. van Steensel, 2007 High-resolution mapping reveals links of HP1 with active and inactive chromatin components. PLoS Genet. 3: e38.

Dimitri, P., 1991 Cytogenetic analysis of the second chromosome heterochromatin of Drosophila melanogaster. Genetics 127: 553–564.

Eberl, D. F., L. J. Lorenz, M. B. Melnick, V. Sood, P. Lasko *et al.*, 1997 A new enhancer of position-effect variegation in Drosophila melanogaster encodes a putative RNA helicase that binds chromosomes and is regulated by the cell cycle. Genetics 146: 951–963.

Eissenberg, J. C., and S. C. Elgin, 2014 HP1a: a structural chromosomal protein regulating transcription. Trends Genet. 30: 103–110.

Elgin, S. C., and G. Reuter, 2013 Position-effect variegation, heterochromatin formation, and gene silencing in Drosophila. Cold Spring Harb. Perspect. Biol. 5: a017780.

Fung, J. C., W. F. Marshall, A. Dernburg, D. A. Agard, and J. W. Sedat, 1998 Homologous chromosome pairing in Drosophila melanogaster proceeds through multiple independent initiations. J. Cell Biol. 141: 5–20.

Gatti, M., S. Bonaccorsi, and S. Pimpinelli, 1994 Looking at Drosophila mitotic chromosomes. Methods Cell Biol. 44: 371–391.

Grewal, S. I., and S. C. Elgin, 2002 Heterochromatin: new possibilities for the inheritance of structure. Curr. Opin. Genet. Dev. 12: 178–187.

Hazelrigg, T., and S. Petersen, 1992 An unusual genomic position effect on Drosophila white gene expression: pairing dependence, interactions with zeste, and molecular analysis of revertants. Genetics 130: 125–138.

Hediger, F., and S. M. Gasser, 2006 Heterochromatin protein 1: don't judge the book by its cover! Curr. Opin. Genet. Dev. 16: 143–150.

Hines, K. A., D. E. Cryderman, K. M. Flannery, H. Yang, M. W. Vitalini *et al.*, 2009 Domains of heterochromatin protein 1 required for Drosophila melanogaster heterochromatin spreading. Genetics 182: 967–977.

Klenov, M. S., S. A. Lavrov, A. D. Stolyarenko, S. S. Ryazansky, A. A. Aravin *et al.*, 2007 Repeat-associated siRNAs cause chromatin silencing of retrotransposons in the Drosophila melanogaster germline. Nucleic Acids Res. 35: 5430–5438.

Lavrov, S. A., A. S. Shatskikh, M. V. Kibanov, and V. A. Gvozdev, 2013 Correlation on a cellular level of gene transcriptional silencing and heterochromatin compartment dragging in case of PEV-producing eu-heterochromatin rearrangement in Drosophila melanogaster. Mol. Biol. 47: 286–291 (in Russian).

Lohe, A. R., A. J. Hilliker, and P. A. Roberts, 1993 Mapping simple repeated DNA sequences in heterochromatin of Drosophila melanogaster. Genetics 134: 1149–1174.

Martin-Morris, L. E., A. K. Csink, D. R. Dorer, P. B. Talbert, and S. Henikoff, 1997 Heterochromatic trans-inactivation of Drosophila white transgenes. Genetics 147: 671–677.

Moshkovich, N., P. Nisha, P. J. Boyle, B. A. Thompson, R. K. Dale *et al.*, 2011 RNAi-independent role for Argonaute2 in CTCF/CP190 chromatin insulator function. Genes Dev. 25: 1686–1701.

Nisha, P., J. L. Plank, and A. K. Csink, 2008 Analysis of chromatin structure of genes silenced by heterochromatin in trans. Genetics 179: 359–373.

Pal-Bhadra, M., B. A. Leibovitch, S. G. Gandhi, M. Rao, U. Bhadra *et al.*, 2004 Heterochromatic silencing and HP1 localization in Drosophila are dependent on the RNAi machinery. Science 303: 669–672.

Sage, B. T., J. L. Jones, A. L. Holmes, M. D. Wu, and A. K. Csink, 2005 Sequence elements in cis influence heterochromatic silencing in trans. Mol. Cell. Biol. 25: 377–388.

Schotta, G., A. Ebert, V. Krauss, A. Fischer, J. Hoffmann *et al.*, 2002 Central role of Drosophila SU(VAR)3-9 in histone H3–K9 methylation and heterochromatic gene silencing. EMBO J. 21: 1121–1131.

Schotta, G., A. Ebert, and G. Reuter, 2003 SU(VAR)3-9 is a conserved key function in heterochromatic gene silencing. Genetica 117: 149–158.

Shidlovskii, Y. V., A. N. Krasnov, J. V. Nikolenko, L. A. Lebedeva, M. Kopantseva *et al.*, 2005 A novel multidomain transcription coactivator SAYP can also repress transcription in heterochromatin. EMBO J. 24: 97–107.

Shpiz, S., S. Lavrov, and A. Kalmykova, 2014 Combined RNA/DNA fluorescence in situ hybridization on whole-mount Drosophila ovaries. Methods Mol. Biol. 1093: 161–169.

Spofford, J. B., 1976 Position-effect variegation in *Drosophila*, pp. 955–1018 in *The Genetics and Biology of Drosophila*, M. Ashburner, and E. Novitski, eds. Academic Press, New York.

Talbert, P. B., and S. Henikoff, 2006 Spreading of silent chromatin: inaction at a distance. Nat. Rev. Genet. 7: 793–803.

Thakar, R., and A. K. Csink, 2005 Changing chromatin dynamics and nuclear organization during differentiation in Drosophila larval tissue. J. Cell Sci. 118: 951–960.

Tulin, A. V., N. M. Naumova, A. A. Aravin, and V. A. Gvozdev, 1998 Repeated, protein-encoding heterochromatic genes cause inactivation of a juxtaposed euchromatic gene. FEBS Lett. 425: 513–516.

Vogel, M. J., L. Pagie, W. Talhout, M. Nieuwland, R. M. Kerkhoven *et al.*, 2009 High-resolution mapping of heterochromatin redistribution in a Drosophila position-effect variegation model. Epigenet. Chromatin 2: 1.

Communicating editor: J. A. Birchler

GENETICS

Supporting Information
www.genetics.org/lookup/suppl/doi:10.1534/genetics.115.181693/-/DC1

The Differences Between *Cis*- and *Trans*-Gene Inactivation Caused by Heterochromatin in *Drosophila*

Yuriy A. Abramov, Aleksei S. Shatskikh, Oksana G. Maksimenko, Silvia Bonaccorsi, Vladimir A. Gvozdev, and Sergey A. Lavrov

DOI: 10.1534/genetics.115.181693

Table S1
List of transgene-bearing fly lines used for trans-inactivation checks and brief description of transgenes used.

Table S2
List of primers and synthetic DNA fragments used in this study.

Table S3
RNA-seq and qPCR numeric data for the genes mentioned in the manuscript.

Table S4
List of genes and their allels tested for the effects on cis- and trans-inactivation.

Table S5
Comparison of expresson levels of genes near the A4 breakpoint in wild-type larvae and the degree of cis-inactivation of these genes in A4/A4 larvae.

Stock number	INSERTED ELEMENT	Trans-inactivation	DIST FROM BP	Position	LOCATION STRAND	INSERTED ELEMENT SIZE	AFFECTED GENES	FBID	STOCK	
12451	*P{GT1}*	No	-532024	chr2L:20650190-20650191	1	8.447	*CG2611*	FBti0017194	12451 w[1118]; P{GT1}CG2611[BG00938]	
12591	*P{GT1}*	No	-329676	chr2L:20852538-20852539	1	8.447	*CG9335*	FBti0017668	12591 w[1118]; P{GT1}BG01978	
12406	*P{GT1}*	No	-264337	chr2L:20917877-20917878	-1	8.447	*Mtp*	FBti0017147	12406 w[1118]; P{GT1}sky[BG00162]	
15527	*P{EPgy2}*	No	-211282	chr2L:20970932-20970933	1	10.908	*CG9266*	FBti0027093	15527 y[1] w[67c23]; P{EPgy2}CG42238[EY01654]	
16715	*P{EPgy2}*	No	-196068	chr2L:20986146-20986147	1	10.908	*CG42238*	FBti0039322	16715 y[1] w[67c23]; P{EPgy2}CG42238[EY06338]	
16113	*PBac{5HPw[+]}*	No	-168014	chr2L:21014191-21014201	1	6.938	*CG42238*	FBti0037689	16113 y[1] w[1118]; PBac{5HPw[+]}CG42238[A428]/CyO	
20390	*P{wHy}*	No	-130760	chr2L:21051454-21051455	1	15.588	*CG42238*	FBti0072674	20390 y[1] w[67c23]; P{wHy}CG42238[DG04612]	
12532	*P{GT1}*	No	-129214	chr2L:21053000-21053001	1	8.447	*betaInt-nu*	FBti0018406	12532 w[1118]; P{GT1}betaInt-nu[BG01037]	
19146	*P{XP}*	No	-112170	chr2L:21070044-21070045	1	7.303	*CG9265*	FBti0042742	19146 w[1118]; P{XP}CG9265[d00690]	
19930	*P{EPgy2}*	No	-79479	chr2L:21102735-21102736	1	10.908	-	FBti0039942	19930 y[1] w[67c23]; P{EPgy2}EY08505	
20292	*P{EPgy2}*	No	-73675	chr2L:21108539-21108540	1	10.908	*Nhe2*	FBti0040222	20292 y[1] w[67c23]; P{EPgy2}Nhe2[EY11323]	
19582	*P{EP}*	Yes+	-40312	chr2L:21141902-21141903	-1	7.987	*Dap160*	FBti0011223	19582 w[1118]; P{EP}Dap160[EP2543]	
SH0471	*P{lacW}*	Yes+++	-38603	chr2L:21143267-21143612	-	10.691	*l(2)SH0471*	FBti0026226	-	
19661	*P{EPgy2}*	Yes++	-38947	chr2L:21143267-21143268	1	10.908	*CG9253*	FBti0039673	19661 y[1] w[67c23]; P{EPgy2}CG9253[EY02880]/CyO	
18010	*PBac{RB}*	Yes+	-34702	chr2L:21147512-21147513	-1	5.971	*del*	FBti0041560	18010 w[1118]; PBac{RB}del[e02039]/CyO	
SH2164	*P{lacW}*	Yes+++	-33283	chr2L:21148427-21148932	-	10.691	*l(2)SH2164*	FBti0025696	-	
SH0354	*P{lacW}*	Yes++	-25866	chr2L:21156176-21156349	-	10.691	*l(2)SH0354*	FBti0026288	-	
17314	*P{EPgy2}*	Yes+++	-25978	chr2L:21156236-21156237	-1	10.908	*E2f2*	FBti0038690	17314 y[1] w[67c23]; P{EPgy2}E2f2[EY02995]	
5329_1	*P{lacW}*	Yes+++	-25316	chr2L:21156898-21156899	-	10.691	*Mpp6*	FBti0018471	5329 y[1] w[67c23]; P{lacW}Mpp6[k16403] P{lacW}k16403b/CyO	
18383	*PBac{WH}*	Yes+/-	-23565	chr2L:21158649-21158650	1	7.234	*CG9249*	FBti0041950	18383 w[1118]; PBac{WH}CG9249[f00877]	
18375	*PBac{WH}*	Yes+	-23562	chr2L:21158652-21158653	-1	7.234	*CG9249*	FBti0041942	18375 w[1118]; PBac{WH}CG9249[f00835]/CyO	
SH2113	*P{lacW}*	Yes+++	-19202	chr2L:21162912-21163013	-	10.691	*l(2)SH2113*	FBti0025712	-	
16587	*P{EPgy2}*	Yes++	-19191	chr2L:21163023-21163024	-1	10.908	*CG9247*	FBti0039166	16587 y[1] w[67c23]; P{EPgy2}CG9247[EY04057]	
10662	*P{lacW}*	No	-18553	chr2L:21163661-21163662	1	10.691	*l(2)k07215*	FBti0006703	10662 y[1] w[67c23]; P{lacW}l(2)k07215[k07215]/CyO	
EP2348	*P{EP}*	Yes++	-18545	chr2L:21163669-21163670	-1	7.987	*CG9246*	FBti0016413	-	
SH0608	*P{lacW}*	Yes+++	-13277	chr2L:21168651-21168938	-	10.691	*Acon*	FBti0026168	-	
20708	*P{EPgy2}*	Yes+++	-13551	chr2L:21168663-21168664	-1	10.908	*Acon*	FBti0057677	20708 y[1] w[67c23]; P{EPgy2}Acon[EY11898]/CyO	
20250	*P{EPgy2}*	Yes++	-2567	chr2L:21179647-21179648	-1	10.908	*bur*	FBti0040180	20250 y[1] w[67c23]; P{EPgy2}bur[EY11080]/CyO	***A4 breakpoint***
43099	*Mi{MIC}*	Yes+++	12958	chr2L:21195076-21195077	-1	7.267	*Ret*	FBti0150551	43099 y[1] w[*]; Mi{y[+mDint2]=MIC}Ret[MI07200]/SM6a	
20229	*P{EPgy2}*	Yes+++	23569	chr2L:21205783-21205784	-1	10.908	-	FBti0040159	20229 y[1] w[67c23]; P{EPgy2}EY10934	
19922	*P{EPgy2}*	Yes+++	24119	chr2L:21206333-21206334	1	10.908	-	FBti0039934	19922 y[1] w[67c23]; P{EPgy2}EY07947/CyO	
20872	*P{EPgy2}*	Yes+++	24168	chr2L:21206382-21206383	-1	10.908		FBti0057845	20872 y[1] w[67c23]; P{EPgy2}EY13357	
10879	*P{lacW}*	Yes+++	32953	chr2L:21215167-21215168	1	10.691	*snRNA:U4:39B*	FBti0006577	10879 y[1] w[67c23]; P{lacW}snRNA:U4:39B[k09410] CG8678[k09410]/CyO	
20175	*P{EPgy2}*	Yes+++	39066	chr2L:21221280-21221281	1	10.908	-	FBti0040078	20175 y[1] w[67c23]; P{EPgy2}EY08386	
SH0778	*P{lacW}*	Yes+++	39751	chr2L:21221701-21221966	-	10.691	*CG8677*	FBti0026091	-	
EP838	*P{EP}*	Yes+++	39814	chr2L:21222028-21222029	1	7.987	*CG8677*	FBti0010729	-	
20152	*P{EPgy2}*	TransActivation	55057	chr2L:21237271-21237272	1	10.908	*Hr39*	FBti0040055	20152 y[1] w[67c23]; P{EPgy2}Hr39[EY04579]	
55A12	*P{w+ 6STe} Hr39*	TransActivation	55064	chr2L:21237278-21237279	-1		*Hr39*			
EP2490	*P{EP}*	TransActivation	55621	chr2L:21237835-21237836	1	7.987	*Hr39*	FBti0011178	-	
DHR39	*P{lacW}*	No	71339	chr2L:21238567-21253554	1	10.691	*EcoI\lacZ*	FBti0007257	-	
12679	*P{GT1}*	No	68555	chr2L:21250769-21250770	1	8.447	*Hr39*	FBti0017714	12679 w[1118]; P{GT1}Hr39[BG02396]	
EP2507	*P{EP}*	No	68583	chr2L:21250797-21250798	-1	7.987	*Hr39*	FBti0021114	-	
11127	*P{lacW}*	Yes+++	79006	chr2L:21261220-21261221	1	10.691	*l(2)k14505*	FBti0006409	11127 y[1] w[67c23]; P{lacW}l(2)k14505[k14505]/CyO	
19694	*P{EPgy2}*	Yes+++	79335	chr2L:21261549-21261550	1	10.908	*l(2)k14505*	FBti0039706	19694 y[1] w[67c23]; P{EPgy2}l(2)k14505[EY04514]/CyO	
SH0764	*P{lacW}*	Yes++	80830	chr2L:21262995-21263045	-	10.691	*l(2)SH0764*	FBti0026097	-	
11019	*P{lacW}*	No	81125	chr2L:21263339-21263340	1	10.691	*l(2)k11226*	FBti0006484	11019 y[1] w[67c23]; P{lacW}l(2)k11226[k11226]/CyO	
10562	*P{lacW}*	Yes+++	113681	chr2L:21295895-21295896	1	10.691	*l(2)k05106*	FBti0006819	10562 y[1] w[67c23]; P{lacW}l(2)k05106[k05106]/CyO	
20102	*P{EPgy2}*	No	127536	chr2L:21309750-21309751	-1	10.908	*Mio*	FBti0040005	20102 y[1] w[67c23]; P{EPgy2}Mio[EY00908]	
12400	*P{GT1}*	Yes+	128691	chr2L:21310905-21310906	-1	8.447	*crc*	FBti0017141	12400 w[1118]; P{GT1}crc[BG00047]	
21396	*P{EPgy2}*	No	136809	chr2L:21319023-21319024	-1	10.908	*crc*	FBti0057990	21396 y[1] w[67c23]; P{EPgy2}crc[EY12903]	
21432	*P{EPgy2}*	No	157052	chr2L:21339266-21339267	1	10.908	*dimm*	FBti0058026	21432 y[1] w[67c23]; P{EPgy2}dimm[EY14636]	
16407	*P{EPay2}*	No	161687	chr2L:21343901-21343902	-1	10.908	-	FBti0039425	16407 y[1] w[67c23]; P{EPay2}EY07263	
12761	*P{GT1}*	No	197953	chr2L:21380167-21380168	1	8.447	*nrv3*	FBti0115741	12761 w[1118]; P{GT1}nrv3[BG01034]	
20886	*P{EPgy2}*	Yes+	426567	chr2L:21608781-21608782	1	10.908	-	FBti0057859	20886 y[1] w[67c23]; P{EPgy2}EY13580	
SH2339	*P{lacW}*	Yes+	442074	chr2L:21624116-21624289	-	10.691	*Cul-2*	FBti0025648	-	
10579	*P{lacW}*	Yes+	447107	chr2L:21629321-21629322	1	10.691	*Df31*	FBti0006768	10579 y[1] w[67c23]; P{lacW}Df31[k05815]/CyO	
20104	*P{EPgy2}*	Yes++	447798	chr2L:21630012-21630013	-1	10.908	-	FBti0040007	20104 y[1] w[67c23]; P{EPgy2}EY00951	
15680	*P{EPgy2}*	Yes++	450359	chr2L:21632573-21632574	-1	10.908	-	FBti0027253	15680 y[1] w[67c23]; P{EPgy2}EY03838	
20063	*P{EPgy2}*	Yes++	451189	chr2L:21633403-21633404	1	10.908	*Ac3*	FBti0039815	20063 y[1] w[67c23]; P{EPgy2}Ac3[EY10141]	
12762	*P{GT1}*	Yes+++	470980	chr2L:21653194-21653195	1	8.447	-	FBti0018088	12762 w[1118]; P{GT1}BG01382	
19883	*P{EPay2}*	Yes+	476805	chr2L:21659019-21659020	1	10.908	*Cul-2*	FBti0039895	19883 y[1] w[67c23]; P{EPay2}Cul-2[EY09124]	
20683	*P{EPgy2}*	No	495077	chr2L:21677291-21677292	-1	10.908	*CG2225*	FBti0057650	20683 y[1] w[67c23]; P{EPgy2}CG2225[EY11545]	
20499	*P{wHy}*	No	495702	chr2L:21677916-21677917	1	15.588	-	FBti0072810	20499 y[1] w[67c23]; P{wHy}DG29208/SM6a	
10770	*P{lacW}*	No	574612	chr2L:21756826-21756827	1	10.691	*step*	FBti0006650	10770 y[1] w[67c23]; P{lacW}step[k08110]/CyO	
11178	*P{lacW}*	No	646275	chr2L:21828489-21828490	1	10.691	*l(2)k16406*	FBti0006360	11178 y[1] w[67c23]; P{lacW}l(2)k16406[k16406]/CyO	
18789	*PBac{WH}*	No	732242	chr2L:21914456-21914457	-1	7.234	*CG31600*	FBti0042372	18789 w[1118]; PBac{WH}CG31600[f04602]	
17367	*P{EPgy2}*	No	934521	chr2L:22116735-22116736	1	10.908	-	FBti0038737	17367 y[1] w[67c23]; P{EPgy2}EY06734	
15021	*P{EPgy2}*	No	949197	chr2L:22131411-22131412	1	10.908	*CycK*	FBti0024854	15021 y[1] w[67c23]; P{EPgy2}EY00324	
16093	*PBac{5HPw[+]}*	No	977964	chr2L:22160178-22160179	-1	6.938	-	FBti0037669	16093 y[1] w[1118]; PBac{5HPw[+]}A317	

P-element mediated insertions with *mini-white* reporter used for trans-inactivation analysis

Transgene	Number of checked(inactivated) insertions	Comment
P{lacW}	18(13)	*Hsp70* promoter- *mini-white* and *P-transposase -LacZ* fusion, construction works as enhancer trap
P{EP}	5(4)	*mini-white* and combination of TrI binding sites, UAS and *Hsp70* promoter to allow inducible misexpression of gene in element insertion point
P{EPgy2}	27(16)	like P{EP} but contains also *yellow* gene
PBac{RB}	1(1)	piggyBack based construction with *mini-white* , FRT site and splice acceptor site (exon from *Rbp1*)
PBac{WH}	3(2)	piggyBack based construction with *mini-white* , FRT site, UAS at one end and insulator (*Su(Hw)* binding site) at opposite end
P{GT1}	8(2)	contains promoter-less *GAL4* gene, *neoR* gene under *Hsp70* promotor and *mini-white* containing splicing donor site instead of polyadenylation signal
P{wHy}	2(0)	Element for generation of deletions, contains *mini-white* , *yellow* and *hobo* mobile element
PBac{5HPw[+]}	2(0)	piggyBack based construction with *mini-white*
P{XP}	1(0)	*mini-white* , FRT sites flanking UAS, two UAS at both ends and insulator (*Su(Hw)* binding site)

Chr	*Start*	*End*	*tracking_id*	*Strand*	*A12L FPKM*	*A12A FPKM*	*log2(A12)L*	*Log2(A4/A12)L*	*log2(A12)A*	*Log2(A4/A12)A*
chr2L	21102742	21104321	CG9257	+	12.98	19.40	3.70	-0.65	4.28	0.00
chr2L	21104567	21134255	Nhe2	+	17.13	9.29	4.10	-1.07	3.22	-0.07
chr2L	21134438	21142353	Dap160	-	15.82	12.24	3.98	-1.24	3.61	0.25
chr2L	21143228	21145146	CG9253	+	6.30	17.26	2.66	-0.13	4.11	0.27
chr2L	21154292	21156232	E2f2	-	11.93	33.37	3.58	-0.74	5.06	0.19
chr2L	21156873	21157685	Mpp6	+	3.26	9.31	1.70	-0.55	3.22	-0.03
chr2L	21157432	21158588	CG9249	-	6.06	23.05	2.60	0.21	4.53	-0.41
chr2L	21158877	21160783	CG9248	+	37.13	26.59	5.21	-0.49	4.73	-0.13
chr2L	21160635	21163087	Nbr	-	13.13	48.58	3.71	-0.75	5.60	-0.23
chr2L	21163610	21166090	CG9246	+	9.41	42.32	3.23	-0.36	5.40	0.04
chr2L	21166045	21168344	CG43345	-	4.28	7.93	2.10	-0.45	2.99	0.30
chr2L	21168615	21173017	Acon	+	100.40	705.57	6.65	0.81	9.46	-0.01
chr2L	21174382	21179697	bur	-	27.68	54.41	4.79	-0.57	5.77	0.10
chr2L	21212321	21220572	CG8678	-	38.33	8.77	5.26	-1.73	3.13	0.10
chr2L	21216003	21218544	CG8679	-	6.27	8.56	2.65	-1.82	3.10	0.15
chr2L	21221311	21231694	CG8677	+	3.31	3.58	1.72	-1.02	1.84	0.85
chr2L	21237249	21259675	Hr39	+	5.76	1.86	2.53	-2.36	0.90	-0.84
chr2L	21261167	21262411	l(2)k14505	+	19.36	38.38	4.28	-0.33	5.26	0.07
chr2L	21262955	21282514	CG8671	+	13.91	18.91	3.80	-0.94	4.24	-0.26
chr2L	21286077	21310050	Mio	+	10.85	19.19	3.44	-0.37	4.26	0.17
chr2L	21310853	21319527	crc	+	200.70	163.78	7.65	-0.34	7.36	-0.27
chr2L	21344606	21358271	Tsp39D	+	3.15	5.56	1.66	-1.06	2.48	-0.78
chr2L	21371226	21377995	CG8665	+	1.73	2.65	0.79	1.61	1.41	-0.42
chr2L	21379999	21393319	nrv3	+	3.56	27.07	1.83	-0.22	4.76	-0.46
chr2L	21573388	21577103	Lamp1	+	130.47	97.52	7.03	-0.82	6.61	-0.44
chr2L	21578318	21589355	nompB	-	0.08	0.12	-3.69	-1.44	-3.09	-0.42
chr2L	21614231	21623627	CG2201	-	29.55	53.73	4.89	-2.38	5.75	-0.37
chr2L	21624678	21626190	CR43148	+	0.59	0.56	-0.76	-1.52	-0.83	-1.60
chr2L	21626308	21629932	Df31	-	144.26	201.25	7.17	-1.35	7.65	-0.37
chr2L	21632586	21647964	Ac3	+	1.16	1.69	0.22	-0.71	0.76	-0.64
chr2L	21658734	21663698	Cul-2	+	19.90	30.63	4.32	-0.83	4.94	-0.19
chr2L	21663805	21677530	CG2225	-	1.94	1.66	0.95	-1.68	0.73	-1.23
chr2L	21678049	21682116	Ef2b	-	2514.29	3413.46	11.30	-0.09	11.74	-0.16
chr2L	21684102	21729051	CG31619	+	1.26	3.34	0.33	-0.05	1.74	0.27
chr2L	21740040	21757466	step	-	12.73	28.94	3.67	-1.06	4.86	0.00

Scatterplots of log2-transformed ratios of *A4* to *A12* expression levels (Y axis) ver. log2-transformed FPKMs in *A12* (X axis) larvae and adults for genes near the *A4* eu-heterochromatin border. There is no obvious correlation between the expression level of the gene and its sensitivity to cis-inactivation by heterochromatin

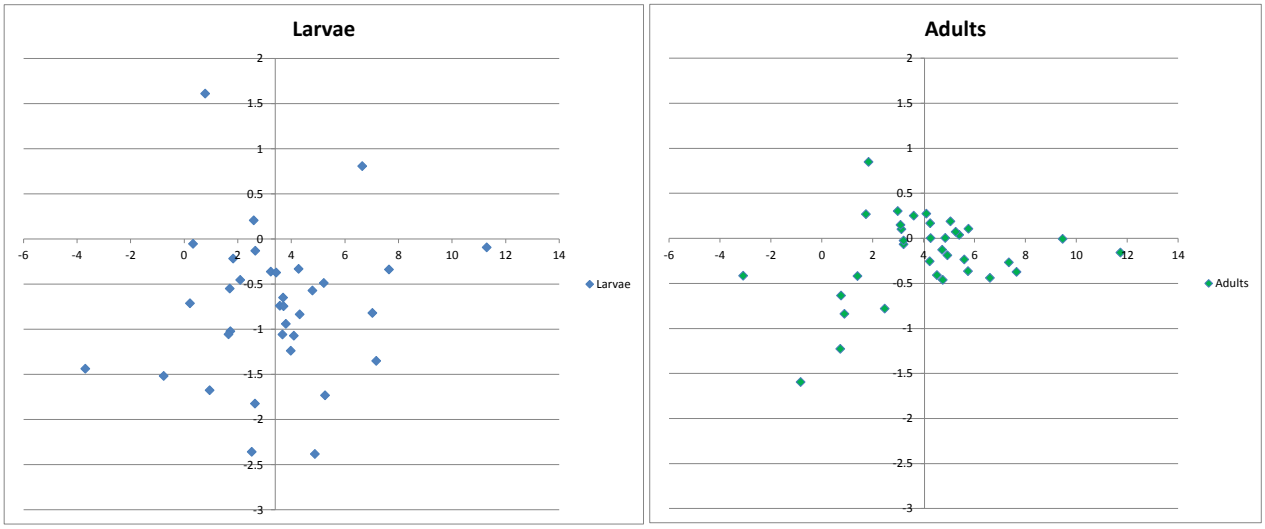

Gene	Synonim	Allele checked	Allele nature	Gene product function	Effect of mutation on trans-inactivation	Effect of mutation on cis-inactivation
Chromosome X						
e(y)3	*SAYP*	*e(y)3*^{4} *(e(y)3*^{u1}*)*	*Stalker insertion, truncated protein*	Chromatin binding, chromatin remodeling, heterochromatin establishment on chromosome 4	very strong suppression	no effect
zeste		*z*^{1}	*Gain of function, point mutation*	Chromatin binding, transvection	no effect	no effect
Chromosome 2						
Su(var)2-5	*CG8409*	*Su(var)2-5*^{1}	*EMS, loss of function*	HP1a chromodomain protein	very strong suppression	very strong suppression
UAP56	*HEL*	*sz*$^{15'}$*/uap56*^{28}	*hypomorphic*	mRNA nuclear transport	no effect	no effect
eggless	*dSETDB1*	*egg*^{1473}	*EMS, truncated protein*	H3-K9 specific histone methyltransferase activity	strong suppression	strong suppression
piwi	*CG6122*	*piwi*^{2}*/powi*^{Nt}	*hypomorphic*	piRNA binding, tranposon silencing	no effect	no effect
Chromosome 3						
Su(var)3-1	*JIL-1*	*JIL-1*^{1}	*EMS, gain of function*	histone kinase activity (H3-S10 specific), prevents heterochromatin spreading	medium suppression	strong suppression
Su(var)3-6	*Pp1-87B*	*Su(var)3-6*^{01}	*EMS, hypomorphic*	Catalytic subunit of PP1 protein phosphatase. Regulates chromosome condensation and affects mitotic chromosome segregation	strong suppression	strong suppression
Su(var)3-7	*CG8599*	*Su(var) 3-7*^{Df}		DNA binding C2H2-like Zinc finger protein	very strong suppression	strong suppression
Su(var)3-7	*CG8599*	*Su(var) 3-7*^{p12}	*Delta2-3*		very strong suppression	strong suppression
Su(var)3-7	*CG8599*	*Su(var) 3-7*^{p43}	*EMS*		very strong suppression	strong suppression
Su(var)3-9	*CG43664*	*Su(var)3-9*^{1}	*EMS, loss of function*	H3-K9 specific histone methyltransferase	no effect	no effect
Su(var)3-9	*CG43664*	*Su(var)3-9*^{6}	*EMS, X ray*		no effect	no effect
Su(var)3-9	*CG43664*	*Su(var)3-9*^{13}	*EMS, hypomorphic*		no effect	no effect
Su(var)3-9	*CG43664*	*Su(var)3-9*^{22}	*hypomorphic*		no effect	no effect
AGO2	*CG7439*	*AGO2*^{414}	*Delta2-3 hypomorphic*	Argonaute 2 is essential for RNA interference (RNAi), bind to chromatin, possibly participates in insulator functioning	enchancement	weak enchancement
AGO2	*CG7439*	*AGO2*^{51B}	*Delta2-3 hypomorphic*		enchancement	weak enchancement

RNA-Seq *FPKM and log2(A4/A12)*

Chr	Start	End	Middle	Inactivation	Gene	Strand	A12L	SD	A4L	SD	Log2(A4/A12)L	SD	A12A	SD	A4A	SD	Log2(A4/A12)A	SD
chr2L	21102742	21104321	21103531.5	-	*CG9257*	+	10.28	0.71	8.28	0.69	**-0.31**	**0.11**	10.77	0.73	12.59	1.03	**0.23**	0.11
chr2L	21104567	21134255	21119411		*Nhe2*	+	13.57	1.61	8.14	0.16	**-0.74**	**0.10**	5.16	0.04	5.75	0.21	**0.16**	0.03
chr2L	21134438	21142353	21138395.5	+	*Dap160*	-	12.54	2.84	6.70	0.22	**-0.90**	**0.19**	6.79	0.66	9.44	0.18	**0.48**	0.08
chr2L	21143228	21145146	21144187	++	*CG9253*	+	4.99	0.39	5.75	0.36	**0.20**	**0.10**	9.58	2.67	13.52	1.05	**0.50**	0.26
chr2L	21154292	21156232	21155262	+++	*E2f2*	-	9.45	0.96	7.14	0.69	**-0.40**	**0.14**	18.52	1.20	24.64	0.86	**0.41**	0.07
chr2L	21156873	21157685	21157279	+++	*Mpp6*	+	2.58	0.90	2.23	0.56	**-0.21**	**0.45**	5.17	0.44	5.93	1.37	**0.20**	0.23
chr2L	21157432	21158588	21158010		*CG9249*	-	4.80	0.38	6.99	0.41	**0.54**	**0.10**	12.79	1.22	11.26	0.43	**-0.18**	0.10
chr2L	21158877	21160783	21159830		*CG9248*	+	29.42	1.76	26.48	2.40	**-0.15**	**0.11**	14.76	1.59	15.76	1.89	**0.10**	0.16
chr2L	21160635	21163087	21161861	++	*Nbr*	-	10.41	0.93	7.83	0.65	**-0.41**	**0.12**	26.96	1.05	26.77	0.66	**-0.01**	0.05
chr2L	21163610	21166090	21164850	++	*CG9246*	+	7.45	1.30	7.32	0.93	**-0.03**	**0.22**	23.49	4.81	28.17	3.36	**0.26**	0.24
chr2L	21168615	21173017	21170816	+++	*Acon*	+	79.56	2.39	175.75	24.70	**1.14**	**0.12**	391.61	5.45	455.15	1.34	**0.22**	0.01
chr2L	21174382	21179697	21177039.5	++	*bur*	-	21.94	1.31	18.64	1.00	**-0.24**	**0.08**	30.20	3.16	37.93	1.41	**0.33**	0.10
chr2L	21182393	21198745	21190569	+++	*Ret*	-	0.25	0.05	0.33	0.02	**0.43**	**0.17**	0.02	0.00	0.14	0.05	**2.88**	0.44
chr2L	21212321	21220572	21216446.5	+++	*CG8678*	-	30.38	5.70	11.53	0.08	**-1.40**	**0.14**	4.87	0.00	6.10	0.34	**0.33**	0.04
chr2L	21216003	21218544	21217273.5	+++	*CG8679*	-	4.97	0.65	1.77	0.26	**-1.49**	**0.20**	4.75	0.84	6.15	0.69	**0.37**	0.21
chr2L	21221311	21231694	21226502.5	+++	*CG8677*	+	2.62	0.63	1.63	0.43	**-0.69**	**0.37**	1.98	0.47	4.17	0.72	**1.07**	0.30
chr2L	21237249	21259675	21248462	+++	*Hr39*	+	4.56	1.56	1.12	0.07	**-2.02**	**0.30**	1.03	0.07	0.67	0.07	**-0.61**	0.13
chr2L	21261167	21262411	21261789	+++	*l(2)k14505*	+	15.35	1.43	15.40	2.29	**0.01**	**0.18**	21.30	0.22	26.16	5.95	**0.30**	0.17
chr2L	21262955	21282514	21272734.5	-	*CG8671*	+	11.02	2.73	7.25	0.54	**-0.60**	**0.24**	10.50	1.59	10.27	0.29	**-0.03**	0.13
chr2L	21286077	21310050	21298063.5	-	*Mio*	+	8.59	1.28	8.37	0.13	**-0.04**	**0.12**	10.65	1.45	13.97	1.08	**0.39**	0.15
chr2L	21310853	21319527	21315190	+	*crc*	+	159.04	21.92	158.71	8.83	**0.00**	**0.14**	90.90	3.16	88.15	2.33	**-0.04**	0.04
chr2L	21344606	21358271	21351438.5		*Tsp39D*	+	2.50	0.72	1.52	0.27	**-0.72**	**0.34**	3.09	1.10	2.10	0.15	**-0.56**	0.32
chr2L	21371226	21377995	21374610.5		*CG8665*	+	1.37	0.64	5.27	1.13	**1.95**	**0.52**	1.47	0.21	1.28	0.31	**-0.20**	0.28
chr2L	21379999	21393319	21386659		*nrv3*	+	2.82	0.86	3.06	0.16	**0.12**	**0.26**	15.02	0.55	12.73	0.43	**-0.24**	0.05
chr2L	21573388	21577103	21575245.5		*Lamp1*	+	103.39	25.28	73.91	8.89	**-0.48**	**0.27**	54.12	6.15	46.62	0.53	**-0.22**	0.09
chr2L	21578318	21589355	21583836.5		*nompB*	-	0.06	0.01	0.03	0.01	**-1.10**	**0.46**	0.07	0.00	0.06	0.01	**-0.19**	0.15
chr2L	21614231	21623627	21618929		*CG2201*	-	23.42	5.46	5.67	0.63	**-2.05**	**0.25**	29.82	4.12	27.05	0.22	**-0.14**	0.11
chr2L	21626308	21629932	21628120	+	*Df31*	-	114.32	32.36	56.59	1.95	**-1.01**	**0.23**	111.70	35.69	100.67	11.13	**-0.15**	0.32
chr2L	21632586	21647964	21640275		*Ac3*	+	0.92	0.18	0.71	0.02	**-0.38**	**0.17**	0.94	0.04	0.71	0.07	**-0.41**	0.09
chr2L	21658734	21663698	21661216		*Cul-2*	+	15.77	3.12	11.16	0.56	**-0.50**	**0.18**	17.00	1.51	17.41	0.21	**0.03**	0.07
chr2L	21663805	21677530	21670667.5		*CG2225*	-	1.54	0.63	0.61	0.12	**-1.34**	**0.45**	0.92	0.34	0.46	0.03	**-1.00**	0.32
chr2L	21678049	21682116	21680082.5		*Ef2b*	-	1992.42	16.25	2358.33	83.44	**0.24**	**0.03**	1894.55	177.80	1982.43	200.89	**0.07**	0.14
chr2L	21684102	21729051	21706576.5		*CG31619*	+	1.00	0.08	1.21	0.07	**0.28**	**0.10**	1.85	0.22	2.61	0.47	**0.49**	0.22
chr2L	21740040	21757466	21748753	-	*step*	-	10.09	2.50	6.12	0.05	**-0.72**	**0.19**	16.06	2.94	18.81	0.86	**0.23**	0.17

qPCR data *Rpl32* normalized / ***Transgenes at primer pair position***

Gene	A12L	SD	A4L	SD	Log2(A4/A12)L	SD	A12A	SD	A4A	SD	Log2(A4/A12)A	SD	Primer pair	Distance from BP, kb	Insertion	Trans-inactivation degree
CG9257	0.008	0.000	0.009	0.000	**0.16**	**0.00**	**0.01**	**0.00**	**0.02**	**0.00**	**0.24**	0.028	**19930_rt**	79.4	**19930**	-
Nhe2																
Dap160	0.012	0.000	0.011	0.000	**-0.18**	**0.00**	**0.02**	**0.00**	**0.02**	**0.00**	**0.15**	0.055	**19582Spr_19582_rt_as**	40.3	**19582**	+
CG9253	0.013	0.001	0.012	0.001	**-0.14**	**0.15**	**0.05**	**0.01**	**0.04**	**0.01**	**-0.06**	0.235	**19661_rt**	38.9	**19661**	++
E2f2	0.009	0.000	0.008	0.000	**-0.29**	**0.00**	**0.06**	**0.01**	**0.06**	**0.00**	**0.01**	0.159	**17314_rt**	26.4	**17314**	+++
Mpp6	0.003	0.000	0.003	0.000	**0.12**	**0.00**	**0.01**	**0.00**	**0.01**	**0.00**	**-0.37**	0.143	**5329_rt**	25.3	**5329_1**	+++
CG9249																
CG9248																
Nbr	0.007	0.000	0.007	0.000	**-0.07**	**0.05**	**0.06**	**0.02**	**0.06**	**0.00**	**-0.05**	0.266	**16587_rt**	19.4	**16587**	++
CG9246	0.002	0.000	0.002	0.000	**-0.25**	**0.03**	**0.01**	**0.00**	**0.01**	**0.00**	**-0.31**	0.215	**ep2348_rt**	18.5	**EP2348**	++
Acon	0.114	0.011	0.234	0.029	**1.03**	**0.16**	**0.66**	**0.05**	**0.62**	**0.00**	**-0.07**	0.055	**20708_rt**	13.5	**20708**	+++
bur	0.012	0.000	0.014	0.000	**0.16**	**0.00**	**0.04**	**0.00**	**0.04**	**0.00**	**0.03**	0.092	**20250**	2.7	**20250**	++
Ret	0.0003	0.0001	0.0004	0.0000	**0.37**	0.60	0.0002	0.0000	0.0004	0.0000	**0.72**	0.19	**SP1171-ASP1936**	12.7	**43099**	+++
CG8678	0.045	0.007	0.011	0.001	**-2.08**	**0.16**	**0.02**	**0.00**	**0.03**	**0.01**	**1.05**	0.164	**10879_rt**	35.1	**10879**	+++
CG8679	0.022	0.002	0.011	0.001	**-1.03**	**0.16**	**0.02**	**0.00**	**0.02**	**0.00**	**-0.07**	0.175				
CG8677	0.013	0.000	0.009	0.001	**-0.58**	**0.06**	**0.03**	**0.00**	**0.04**	**0.00**	**0.46**	0.054	**ep838_rt**	39.8	**EP838**	+++
Hr39	0.006	0.001	0.002	0.000	**-2.01**	**0.15**	**0.00**	**0.00**	**0.01**	**0.00**	**0.34**	0.053	**Hr39_rt**	63.7	**55A12**	+++
l(2)k14505	0.008	0.000	0.009	0.001	**0.18**	**0.09**	**0.01**	**0.00**	**0.02**	**0.00**	**0.71**	0.030	**11127_rt**	79	**11127**	+++
CG8671	0.029	0.001	0.021	0.001	**-0.48**	**0.09**	**0.04**	**0.00**	**0.03**	**0.00**	**-0.22**	0.067	**11019_rt**	81.1	**11019**	-
Mio	0.008	0.002	0.005	0.000	**-0.69**	**0.14**	**0.01**	**0.00**	**0.01**	**0.00**	**-0.07**	0.092	**20102 spr2+aspr2**	127.5	**20102**	-
crc	0.036	0.006	0.039	0.000	**0.12**	**0.12**	**0.03**	**0.00**	**0.04**	**0.00**	**0.57**	0.013	**12400_rt**	128.6	**12400**	+
Tsp39D																
CG8665	0.0015	0.0004	0.0065	0.0014	**2.11**	0.74	0.0039	0.0002	0.0056	0.0021	**0.54**	0.62	**CG8665_2ex_F-CG8665_2ex_R**			
nrv3																
Lamp1																
nompB	0.0002	0.0000	0.0003	0.0001	**0.64**	0.53	0.0004	0.0000	0.0004	0.0000	**0.01**	0.13	**nompB_4ex_F-nompb_4ex_R**			
CG2201	0.0236	0.0041	0.0182	0.0008	**-0.37**	0.32	0.0296	0.0002	0.0323	0.0007	**0.13**	0.04	**CG2201_F-CG2201_R**		**SH2339**	+
Df31	0.278	0.038	0.203	0.024	**-0.45**	**0.18**	**0.45**	**0.07**	**0.52**	**0.05**	**0.20**	0.176	**10579_rt**	446.6	**10579**	+
Ac3																
Cul-2																
CG2225	0.0068	0.0000	0.0080	0.0017	**0.24**	0.32	0.0041	0.0001	0.0046	0.0004	**0.18**	0.16	**CG2225_F-CG2225_R**		**20683**	-
Ef2b																
CG31619																
step	0.008	0.000	0.005	0.000	**-0.72**	**0.02**	**0.03**	**0.00**	**0.03**	**0.00**	**-0.13**	0.031	**10770_rt**	574.6	**10770**	-

ChIP for HP1a and H3K4me2 in 3rth instar larva, females

		Log2(A4/A12)						
Position	*Gene*	*aH32MetK4*	*SD*	*aHP1*	*SD*	*Insertion*	*Inactiva*	*Primer pair*
21170816	***Acon***	-0.55	0.19	0.27	0.15	**20708**	+++	**20708rt**
21216446.5	***CG8678***	-0.45	0.20	0.59	0.15	**10879**	+++	**10879 rt2ex**
21217273.5	***CG8679***	-0.70	0.12	1.07	0.03	**10879**	+++	**10879_rt_intgen_a**
21237724	***Hr39***	-0.12	0.11	1.40	0.16	**55A12**	+++	**EP2490SprAspr**
21310855	*crc*	-0.19	0.18	0.14	0.14	**12400**	+	**12400rt**

Primers for trans-inactivated region												Comments
			Sence primer				Antisence primer					
Primer pair	Gene	Chr	Start	End	ID	Sequence	Start	End	ID	Sequence		
19930Spr-19930ASpr	*CG9257*	chr2L	21102549	21102578	19930Spr	CAATTCAATAAATAAAAAGAACGCACGCA	21102746	21102781	19930ASpr	CGGAATAAATCCATTTACAAACTCGTATAGAAATA		
19930_rt_s-19930_rt_as	*CG9257*	chr2L	21102753	21102782	19930_rt_s	ATACGAGTTTGTAAATGGATTTATTCCGG	21103054	21103079	19930_rt_as	GCGTTGACCGCGTATATAACTTTCA		
20292Spr_1-20292ASpr_1	*Nhe2*	chr2L	21108472	21108504	20292Spr_1	TAGACCATCTTCTATATTTTTCACGTTTCCAC	21108668	21108700	20292ASpr_1	CCAGCAACAATTACAAATGTTTTCTATGTAGG		
19582Spr-19582_rt_as	*Dap160*	chr2L	21141834	21141860	19582Spr	TTATCGTCCTTTTCCGTATGCGTGT	21141976	21142001	19582_rt_as	AAATCCATTGTGAAAATTTGTGGGG		
19661_rt_s-19661_rt_as	*DmRH24*	chr2L	21143259	21143285	19661_rt_s	TGGTAATGTCCGTACCGTGAAATTTT	21143426	21143453	19661_rt_as	CTTTATCATCTTCACCACTTAGTGCCG		
deadlockASP-deadlockSP	*deadlock*	chr2L	21145570	21145598	deadlockASP	CAAATTTATCTGAGCAGTCTACGGAGGA	21145728	21145753	deadlockSP	TGCCATGCAAAGCTCACAAATATCG		
18010Spr-18010ASpr	*deadlock*	chr2L	21147369	21147392	18010Spr	GAAAGCGGCAGTTGGTCATCAGA	21147560	21147587	18010ASpr	GTTGGTCAGACGCAAGATTACAAAGCT		
17314_rt_s-17314_rt_as	*dE2F2*	chr2L	21155755	21155777	17314_rt_s	GATGGATCCTTCGTTGGCCTTC	21155937	21155959	17314_rt_as	GATTCGGCTGAGACTTCGGTCC		
5329_rt_s-5329_rt_as	*Mpp6*	chr2L	21156881	21156910	5329_rt_s	GAAAAAAATTAAATGTGCCTGATGGTTTC	21157094	21157121	5329_rt_as	TGGAATTGAGCATCTTCTGGTTGATCT		
16587_rt_s-16587_rt_as	*Nbr*	chr2L	21162710	21162730	16587_rt_s	TCAGGGCCAGGAGCAAAGGA	21162902	21162925	16587_rt_as	GAGCAACCTGAAGATCAAGCGCT		
ep2348_rt_s-ep2348_rt_as	*CG9246*	chr2L	21163629	21163650	ep2348_rt_s	CCCGTTGAACAGCACACGTGC	21163811	21163832	ep2348_rt_as	CGGCGACTTTCTGCTTCGGGT		
20708_rt_s-20708_rt_as	*Acon*	chr2L	21168651	21168681	20708_rt_s	TTTAGTCTGTCTTAAAATCTTCCGGCTGAG	21168768	21168790	20708_rt_as	TCATCAATCTCGCAGCCATGGT		
20708_2ndex_s-20708_2ndex_as	*Acon*	chr2L	21170486	21170513	20708_2ndex_s	ACAGATGGCTCTGCTTCAGTTTATCTC	21170538	21170563	20708_2ndex_as	AATGATCACAGTGAACAGTGGAGGG		
20250Spr-20250ASpr	*bur*	chr2L	21179461	21179486	20250Spr	GTTTTCCTTCCTCACGCACACATC	21179649	21179673	20250ASpr	GGTCATCCGCTCGTCAATAAGTCA		
SP1171-ASP1936	*Ret*	chr2L	21185224	21185256	SP1171	TCTAGGGGATCACAGACATGATCTGGACAGTAA	21185392	21185422	ASP1936	GCGAACTGAAGGTCAAGTCTCGATCACAGAC		
20229Spr-20229ASpr		chr2L	21205620	21205642	20229Spr	ACCGCCGATGACCAAGAACTGT	21205810	21205838	20229ASpr	GACAAACTATACGTCCTGAAACCAATGC		
10879_rt_2ex_s-10879_rt_2ex_as	*Atg18b*	chr2L	21214006	21214027	10879_rt_2ex_s	CTCCACTGGCCGAGAAGACCA	21214140	21214158	10879_rt_2ex_as	TTTCTCGCCCAGCGGAGC		
10879_rt_intgen_s-10879_rt_intgen_as	*dLEM3*	chr2L	21216329	21216351	10879_rt_intgen_s	AACTGTGATTCTCCCTCCGCCA	21216454	21216478	10879_rt_intgen_as	GCTCTGGGCTTGAATCACCTTACC		
ep838_rt_s-ep838_rt_as	*dRsf-1*	chr2L	21221629	21221649	ep838_rt_s	AAGGACGACGACGCCCTCAC	21222493	21222515	ep838_rt_as	GGCGGACTCCCAACTCTTTTCG		
20152Spr-20152ASpr	*Hr39*	chr2L	21237113	21237135	20152Spr	AGTAACCCACCGTCGCTGCCTT	21237299	21237322	20152ASpr	AATCCGATTCCACAACCGCTCTA		
EP2490Spr-EP2490ASpr	*Hr39*	chr2L	21237724	21237747	EP2490Spr	TGCGTGTGAGTGACCCGTTTACC	21237915	21237940	EP2490ASpr	GCTCTTGTTGCGTTTTCCTCACCTT		
Hr39_rt_s-Hr39_rt_as	*Hr39*	chr2L	21238409	21238439	Hr39_rt_s	AATGTGACTAGAATGTGAGTCGAACAAAAC	21253591	21253620	Hr39_rt_as	TTCTCAGTTGTGCAATTTGTAAAAGTTTG		
EP2507Spr-EP2507ASpr	*Hr39*	chr2L	21250772	21250796	EP2507Spr	AACCCCAAAAAAAGATAGCCAGCG	21250956	21250980	EP2507ASpr	CCAACAACAACCATAGCGACGACA		
11127_rt_s-11127_rt_as	*l(2)k14505*	chr2L	21261169	21261198	11127_rt_s	CACTGAAAACTCAACTCTGCTGTTAAACA	21261266	21261289	11127_rt_as	TGAAATTGGTCAACCGGAGAGCT		Pair denoted as 11127 in ChIP experiment
11019_rt_s-11019_rt_as	*CG8671*	chr2L	21262989	21263013	11019_rt_s	GCATCATCGGTGGTATTCTGTTGC	21263655	21263678	11019_rt_as	GCCATTTACACTTTCCGCACGAA		
11019Spr_3-11019ASpr_3	*CG8671*	chr2L	21263232	21263257	11019Spr_3	GAGGCATACATTTTCCCAGTCGCTT	21263405	21263434	11019ASpr_3	CGAGATTGTTATATTCACACACACGCTTT		
20102Spr_2-20102ASPr_2	*Mio*	chr2L	21309657	21309682	20102Spr_2	CAGATGTCAGGCAGCAATGTTGTCC	21309861	21309887	20102ASPr_2	GCAGTTGCAGTTGTACCGAAATTGTG		
12400_rt_s-12400_rt_as	*crc*	chr2L	21310855	21310881	12400_rt_s	TGATTCCAACACTCATTACCGTTCCA	21310922	21310952	12400_rt_as	GCCATCTTTAGGTTAATATAAATGCCGAAA		
CG8665_2ex_F-CG8665_2ex_R	*CG8665*	chr2L	21374324	21374343	CG8665_2ex_F	GGGCTACCCTGAATGTGTTG	21374413	21374432	CG8665_2ex_R	TGACGTGGGAGGATAGAAGG		
nompB_4ex_F-nompb_4ex_R	*nompB*	chr2L	21586567	21586586	nompB_4ex_F	TTCAGTTTACCGCCACCTTC	21586733	21586753	nompb_4ex_R	TTCGGAGACTTTGTGATGTCC		
CG2201_F-CG2201_R	*CG2201*	chr2L	21615144	21615163	CG2201_F	ACCAAAGGCTCCAGAACAGA	21615302	21615322	CG2201_R	CTTCTACCACAACTCCAGCAA		
10579_rt_s-10579_rt_as	*Df31*	chr2L	21628069	21628092	10579_rt_s	CCTTGGCTACGCTCTCCTCTTCG	21629721	21629742	10579_rt_as	CGTGTTTTCTCGCTTCGCGTT		
CG2225_F-CG2225_R	*CG2225*	chr2L	21668997	21669016	CG2225_F	AAATTCTAGCACCCGCTTTG	21669093	21669112	CG2225_R	CTTTGTTGCGTGGAGACCTT		
10770_rt_s-10770_rt_as	*step*	chr2L	21756571	21756591	10770_rt_s	TTCCTGCTTCTTGCGTCGCA	21757187	21757212	10770_rt_as	AGATCGTACGGTGCCATATCAAAGG		
10770Spr-10770ASpr	*step*	chr2L	21756671	21756698	10770Spr	TTCTGGGCATTTTGTAAATTGTATCGC	21756848	21756873	10770ASpr	AGCAATCCATTGTGGTTTCGACAAG		
Other used primers												
60Ds6-60Das6		chr2R	20322298	20322317	60Ds6	TTCCCCATCCTCGAGCCCTG	20322447	20322469	60Das6	CCAGCCGAGACGAGCACCATAAT		Used for sample quantity normalisation in ChIP experiments
Rp49up-Rp49rev2	*Rpl32*	chr3R	25871481	25871501	Rp49up	ATGACCATCCGCCCAGCATAC	25871414	25871436	Rp49rev2	GCTTAGCATATCGATCCGACTGG		Used for sample quantity normalisation in RT-qPCR experiments
His1 coding s1-His3 coding as1	*His1-4*	chr2L			His1 coding s1	CGTCCGCTTCCCCAGTGG			His3 coding as1	CCTGAGCGATTTCACGCACCA		Used for synthesis of fluorescent probe to histone genes cluster
miniwht_1int_s-miniwht_1int_as	*white*	chrX	2687189	2687216	miniwht_1int_s	AACTACAAGCGTTATGCTCATCTAACCC	2689961	2690063	miniwht_1int_as	TCTAAAGGCATTCATTTTCGACTACATTCT		Probe for *mini-white* gene in ChIP experiments
DSG3-DSG4	*LacZ*				DSG3	TCTCTATCGTGCGGTGGTTGA			DSG4	GCGGATGGTTCGGATAATGC		Probe for *LacZ* gene in ChIP experiments
					Biot-AACAC	Biot-(AACAC)x8						Biotinilated probes for satellite DNA
					Biot-AATAACATAG	Biot-(AATAACATAG)x5						Biotinilated probes for satellite DNA
		chr2L	21150730	21150759	S39C1150540	AAACAAATCAAACCCGAGAAAGCAACGCA						Primers used for *A4* breakpoint mapping and probe synthesis
		chr2L	21156851	21156880	AS39C8849	AAAGCAGAATGACCGAGCACAACAAATGG						Primers used for *A4* breakpoint mapping and probe synthesis
		chr2L	21158849	21158878	SP39C66254	GACTGTCAGCAGGAACCAATGGAATGGAG						Primers used for *A4* breakpoint mapping and probe synthesis
		chr2L	21166230	21166253	AS39C1150540	GAAGAAACGCAACGCCGCCGAAT						Primers used for *A4* breakpoint mapping and probe synthesis
		chr2L	21167355	21167383	SBP39C1419	GCGGTCTTCTTTGATTGATGTGCGTGTG						Primers used for *A4* breakpoint mapping and probe synthesis
		chr2L	21173423	21173453	AS39C5453	AAGTGTAGGAGCCTGTGCTGGAGTCAAAGG						Primers used for *A4* breakpoint mapping and probe synthesis
		chr2L	21176947	21176971	SBP39C11116	ACGGACTGTGTGCGACTGAGGCGA						Primers used for *A4* breakpoint mapping and probe synthesis
		chr2L	21181387	21181416	S39C1181389	CTAACCACACCTCAAAGCCCAAAACAGCC						Primers used for *A4* breakpoint mapping and probe synthesis
		chr2L	21181387	21181416	ASBP39C1419	GGCTGTTTTGGGCTTTGAGGTGTGGTTAG						Primers used for *A4* breakpoint mapping and probe synthesis
		chr2L	21183463	21183488	AS39C1181389	CAACGGGCAGGTTTTGCGATACGAA						Primers used for *A4* breakpoint mapping and probe synthesis
		chr2L	21183486	21183511	SBP39C17560	TGGCGGTAGCATCAAGCAAAGGTCG						Primers used for *A4* breakpoint mapping and probe synthesis
		chr2L	21187542	21187572	ASBP39C18124	GCAACGGAATAGAAACGGGAACAACAAGTG						Primers used for *A4* breakpoint mapping and probe synthesis
		chr2L	21187736	21187764	SP39C6847	CGTGGTAATAGCGTCTGGCAGGGAAAGC						Primers used for *A4* breakpoint mapping and probe synthesis
		chr2L	21196811	21196845	S39C1196813	AGACCGAGAGACCGACTAACTGACTGACTGACTG						Primers used for *A4* breakpoint mapping and probe synthesis
		chr2L	21196811	21196845	ASBP39C17560	CAGTCAGTCAGTCAGTTAGTCGGTCTCTCGGTCT						Primers used for *A4* breakpoint mapping and probe synthesis
		chr2L	21199728	21199752	SP39C1202044	TTGCAGCCGGCACAGGTGTAGGTG						Primers used for *A4* breakpoint mapping and probe synthesis
		chr2L	21203030	21203060	SP39C1019	GGGAGGTCTTCCACTTTCAAGGGTGATTTC						Primers used for *A4* breakpoint mapping and probe synthesis
		chr2L	21203991	21204017	ASP39C1204735	CACACATTGCTGTGCTCCACCGAGTG						Primers used for *A4* breakpoint mapping and probe synthesis
		chr2L	21204167	21204194	AS39C1204815	CGCCTGACACAAATTCCCATCCGACTT						Primers used for *A4* breakpoint mapping and probe synthesis
		chr2L	21210234	21210262	4_inversion_region_al	GCCGAGGATCTGGCTGCACAAAGTAAAA						Primers used for *A4* breakpoint mapping and probe synthesis
		chr2L	21210992	21211018	AS39C1196813	TGAAAGCAAGCCGAGACCAAGCACCA						Primers used for *A4* breakpoint mapping and probe synthesis
		chr2L	21218750	21218780	4_inversion_region_al	GCGCAACACGTGTTGTTGCTATTTCTGACT						Primers used for *A4* breakpoint mapping and probe synthesis
		chr2L	21218847	21218876	i4_inversion_region_a	CTCAATGCGCTATCGCATAACAAGGGGTA						Primers used for *A4* breakpoint mapping and probe synthesis
		chr2L	21226988	21227015	4_inversion_region_al	GGCAGTCGGCAAGGCTGAAAGGTAAA						Primers used for *A4* breakpoint mapping and probe synthesis
		chr2L	21227005	21227028	i4_inversion_region_a	TCCGCGAAGCCGCTTTACCTTTT						Primers used for *A4* breakpoint mapping and probe synthesis
		chr2L	21235104	21235125	i4_inversion_region_a	CAGAGCGCCGGGTGAGGGTCG						Primers used for *A4* breakpoint mapping and probe synthesis
		chr2L	21235108	21235132	4_inversion_region_al	CCTCACCCGGCGCTCTGCTTATTG						Primers used for *A4* breakpoint mapping and probe synthesis
		chr2L	21244072	21244100	i4_inversion_region_a	ACTGTTCTTGGTGGCTCTGGCTCTCTCG						Primers used for *A4* breakpoint mapping and probe synthesis
		chr2L	21244079	21244109	4_inversion_region_al	GCCAGAGCCACCAAGAACAGTAAAACACG						Primers used for *A4* breakpoint mapping and probe synthesis
		chr2L	21251826	21251850	i4_inversion_region_a	GGAGCGGCGAGGCAATGAAGCAAT						Primers used for *A4* breakpoint mapping and probe synthesis
		chr2L	21251838	21251858	4_inversion_region_al	CCTCGCGCTCCATCGTCGC						Primers used for *A4* breakpoint mapping and probe synthesis
		chr2L	21260077	21260106	i4_inversion_region_a	CGCCCATTCTATAGCCCTAAAACCGCAAA						Primers used for *A4* breakpoint mapping and probe synthesis
		chr2L	21210832	21210858	S39C71	ATCAGTGCGGCAGTGCTGAAGTTGGG						Primers used for *A4* breakpoint mapping and probe synthesis
		chr2L	21218352	21218379	AS39C71	CCCTGGAGGACGAGAACGAGGCTGATA						Primers used for *A4* breakpoint mapping and probe synthesis